

Politecnico di Torino

Dipartimento di Ingegneria Meccanica e Aerospaziale

Corso di Laurea Magistrale in Ingegneria Biomedica

Development of a Barrier-On-Chip model and fabrication of embedded high-resolution porous-membrane based electrodes to assess the integrity of the barrier

Tesi di Laurea Magistrale in Ingegneria Biomedica

Studente

Antonio Martino

Relatori

Prof. Gianluca Ciardelli

Prof. Peter Ertl

Anno Accademico 2021-2022

Ai miei genitori

Table of Content

Abstract	6
Aim	7
1	
Introduction	8
1.1 Organ-On-Chip Technology	16
1.1.1 Main aspects of a Microdevice	17
1.1.2 MEMS and Bio-MEMS	19
1.1.3 Lab-On-Chip and Microfluidics Devices	20
1.1.4 Organ-On-Chip Devices	22
1.2 Advantages of a Microfluidics Device	Error! Bookmark not defined.
1.3 Evaluation of cell barrier integrity	14
2	
Materials and Methods	25
2.1 Methods	25
2.1.1 Layer-by-Layer Chip Design	25
2.1.2 Mold Chip Design	Error! Bookmark not defined.
2.1.3 Electrodes Fabrication	Error! Bookmark not defined.
2.1.4 Electrodes Validation	Error! Bookmark not defined.
2.1.5 Cell Culture in the chip	44
2.2 Materials	Error! Bookmark not defined.
3	
Results and Discussion	55

3.1	Result-	55
3.2	Discussion.....	75

Abstract

The human body possesses a large variety of barriers, of different origins and characteristics, playing an important role in the functioning of the organism. They are responsible for controlling some essential biological processes and maintaining homeostasis by regulating the interactions between the compartments that they separate. A possible disruption of the barrier can lead to important consequences. It can indeed be associated with severe diseases including multiple sclerosis in the case of disruption of the blood-brain barrier or disorders such as celiac disease in the case of loss of intestinal barrier integrity. Monitoring the status and integrity of a cell barrier is therefore crucial. In-depth analysis of the state of a cell barrier in laboratory requires the employment of accurate in vitro models able to mimic the corresponding in vivo environment with remarkable accuracy. To this purpose, the realization of an OOC (Organ-On-Chip) device capable to mimic a cellular barrier in vitro i.e., a Barrier-On-Chip device, and the fabrication of embedded high-resolution membrane-based gold electrodes to evaluate the integrity of the barrier performing TEER (Trans-Epithelial Electrical Resistance) measurements is proposed. These gold sensors fabricated on top of PET membranes allow for more reproducible and reliable measurements than the classical setup for measuring TEER, where readings are instead performed through chopstick electrodes in a Transwell system. In this study, a stable leakage-free method of manufacture of a dual-chamber PDMS device containing a thin microporous PET middle layer was proposed. The in vitro model was then validated under dynamic flow and static culture conditions of CACO-2 gut cells. Furthermore, a protocol optimization for the fabrication of the embedded membrane-based electrodes was also presented. Specifically, it is proposed a non-aggressive lift-off system to increase the manufacturing efficiency of the sensors. Finally, a proof-of concept in evaluating the integrity of an intestinal barrier in the absence and presence of compounds is also provided.

Keywords: *Organ-on-chip, in vitro barrier models, photolithography, TEER, impedance spectroscopy*

Aim

The aim of this thesis is to propose the fabrication of a Barrier-on-Chip model in PDMS, suitable for deployment in static and dynamic culture to realize an in vitro cell barrier model having a layer composed of a very thin microporous PET membrane to mimic the substance exchanges that occur in vivo in the human body. The optimization of an embedded electrode fabrication protocol for TEER measurement, manufactured by photolithography above the membrane, is also covered in the thesis.

List of Figures

1) Figure 1.1: Schematic illustration of the different type of barrier in the human body, adapted from [1]

List of Tables

1) Table 3.1: Follow-up of the smoothing procedure of the surfaces of PDMS casting molds.

List of Abbreviations

2D	Two-dimensional
3D	Three-dimensional
ID	Internal Diameter
CE	Counter electrode
DMEM	Dulbecco's Modified Eagle's Medium
ECM	Extracellular Matrix
FCS	Fetal Calf Serum
NSAID	Nonsteroidal anti-inflammatory drug
OOC	Organ-On-Chip
PBS	Phosphate buffered solution
PDMS	Polydimethylsiloxane
PET	Polyethylene terephthalate
PFA	Paraformaldehyde
RE	Reference electrode
RPM	Revolutions per minute
RT	Room temperature

UV	Ultraviolet
TEER	Trans-Epithelial Electrical Resistance
TJ	Tight Junctions
TMAH	Tetramethylammonium hydroxide
WE	Working Electrode
Col I	Collagen Type I
ZO-1	Zonula occludent-1

1

Introduction

Before discussing the details of the thesis, an in-depth look at the biological reasons is necessary to understand the final purpose of the thesis and why it is crucial to understand the integrity of a cellular barrier.

1.1 Biological Degression

1.1.1. Role of the Barrier in Human Body

The human body presents different type of barriers. Some of these barriers are exploited as mechanical protections such as the skin, the mucous membranes of respiratory, urinary, or gastrointestinal tracts[2], [3]. These are important part of the innate immune system and represent a first-line barriers to infection, blocking the entry and growth of pathogens [4]. Moreover, within the body, there are microporous barriers that regulate the exchange of substances between two different compartments and they are responsible for maintaining many vital processes such as homeostasis. Some of them, such as the Blood-Brain-Barrier (BBB) or the Blood-Retinal-Barrier (BRB) are also extremely helpful as high-selective filters for certain toxins that may affect vital organs [5].

1.1.2. Importance of structural integrity of a cell barrier

As already mentioned, the barriers in the body are very different and have different functions, but they are united by certain structural features like tight junctions[6]. They are all characterized by junctional complexes where different connectors, proteins play vital roles[7]. The structural maintenance of a barrier is therefore fundamental and at the core of many important human processes, but it can

nevertheless be compromised by inflammatory situations, including minor ones [1]. The maintenance of homeostasis is strongly related to inflammation, it starts at a low cellular level and can escalate in some cases to systemic inflammation after triggering several cascades and involving several organs[8], [9]

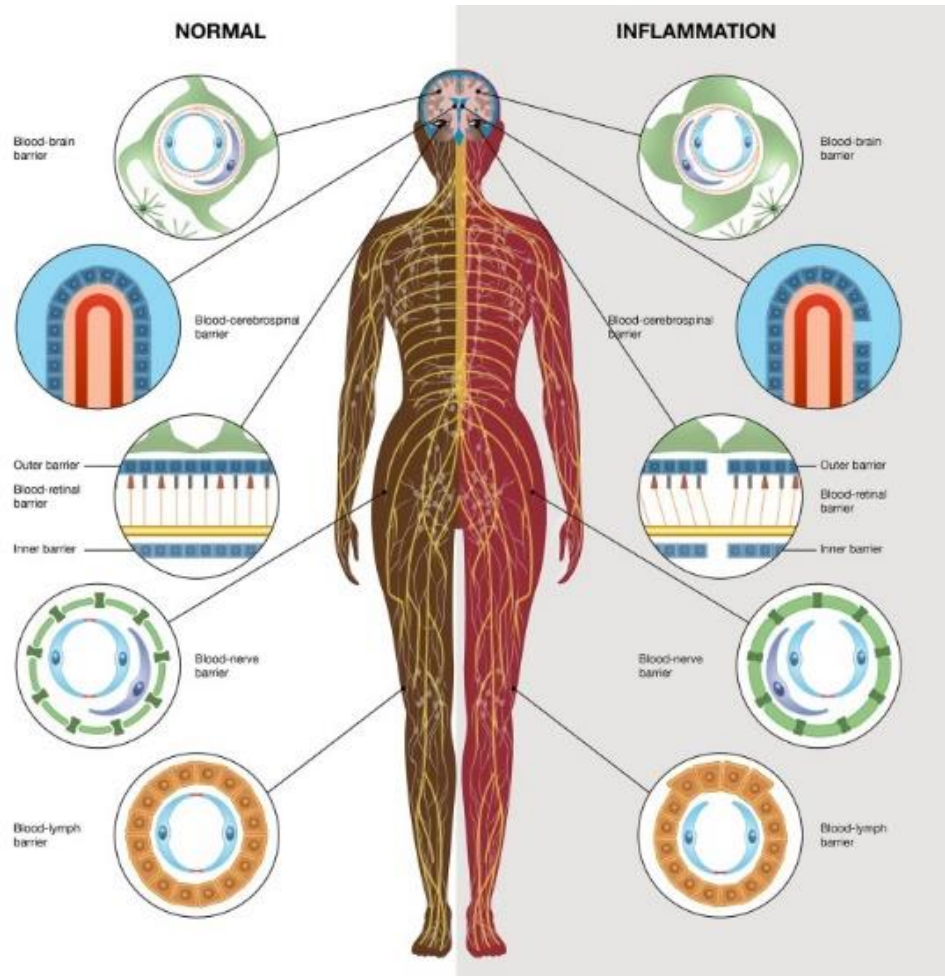


Figure 1.1: Schematic illustration of the different type of barrier in the human body, in particular the Blood-brain barrier (BBB), Blood-cerebrospinal barrier (BCB), the Blood-retinal barrier (BRB), the Blood-nerve barrier (BNB) and the Blood-lymph barrier (BLB). The scheme on the left shows their structure in a normal functioning condition of the body, while on the right the figure shows their configuration in the presence of inflammation. The structures in this case are altered and visibly disrupted[1].

Recent studies have also shown how local inflammatory situations disrupt the balance in gap junction coupled cells. Inflammatory stimuli could modify cell signaling that is altered through connexin-related gap junctions with the result in the dysregulation of cellular networks [10]. Therefore, it is of key relevance to investigate and understand the structural state of a barrier as its disruption can be linked to serious pathologies. For instance, disruption of the Blood Brain Barrier (BBB) could be linked to metabolic disorders such as multiple sclerosis [11], or a malfunction of the Blood Retina Barrier (BRB) could be associated with eye diseases such as macular degeneration [12] (Figure 1.1) or moreover the intestinal barrier integrity loss may be connected to inflammatory bowel pathology or celiac disease[13] and the endothelial barriers in neurodegenerative disorders[14].

1.2 Evaluation of cell barrier integrity

As explained above, disruption of a barrier is strongly linked to other more important pathologies, so it is essential to be able to analyze the integrity of a barrier to understand how cells arrange themselves and how exchanges between the two compartments are regulated to recognize any abnormal behaviour in certain situations.

1.2.1 Cell Barrier Layer In Vitro

Talk about how the biological reason how cells grow to form a barrier, the standard measurement of the barrier integrity and what we can really measure to assess this barrier, should I also insert here the impedance electrodes and the news that they bring??.

The use of porous membrane and what they allow (Use of porous membranes in tissue barrier), all the properties (they allow cell-cell interaction, talk about optical transparency, thin membrane)[15]

These devices, need accurate sensors to carry out direct measurements on cell culture to be as close as possible to the in vivo organ. For these reasons, in this work, it is proposed the fabrication of electrodes able to perform TEER (Trans-Epithelial Electrical Resistance) measurements that allow to execute reliable impedance measurements capable of controlling the integrity of a cellular

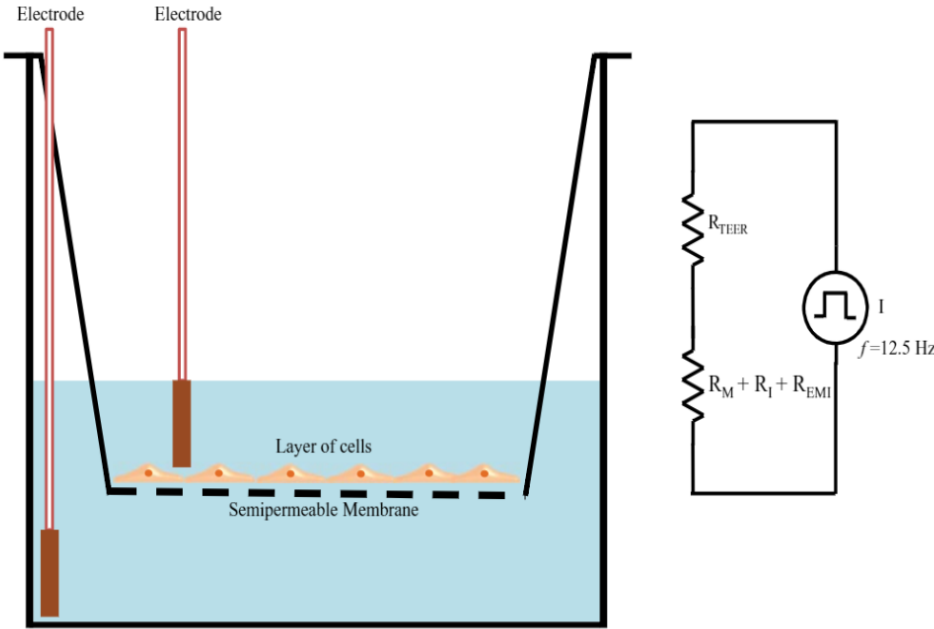
barrier with higher precision than the models on the market. The electrodes were fabricated using high-resolution photolithography process that were integrated into a previously fabricated gut-on-a-chip model to ensure their effectiveness for the final purpose.

The electrodes were fabricated using high-resolution photolithography process that were integrated into a previously fabricated gut-on-a-chip model to ensure their effectiveness for the final purpose. The manufacture of the chip mentioned above is also subject of this thesis. The electrodes are fabricated directly on top of the membrane used as the intermediate layer. This represents a major innovation and considerable utility of these systems, since they are fabricated directly on the membrane, unlike the usual metal electrodes which are fabricated on glass. The manufacturing method therefore allows direct integration of the electrode into the chip. The presence of the in-situ electrodes is extremely important as it allows measurements to be made on the efficiency of the cell barrier formed during the period of cell culture inside the chip. In fact, usually the validation of the integrity of the cell barrier that has been formed during the cell culture, is carried out through open systems such as the Transwell system where cells grow in a porous membrane that is in the middle of two chambers with two independent accesses. In this case, measurements are made through chopstick electrodes introduced from outside by performing TEER measurements. Instead, the presented system in this work, allows integrity and permeability test of the barrier performing impedance measurements through electrodes integrated directly inside the chip. This allows real time measurements to be performed during the culture that takes place inside the chip and it is also conducted in a more stable and efficient manner as the electrodes are integrated on the chip.

1.2.2 TEER measurement standard

Chopstick electrodes inside a Transwell system

The use of porous membrane and what they allow (Use of porous membranes in tissue barrier), all the properties (they allow cell-cell interaction, talk about optical transparency, thin membrane)[15]



The sensors that are commonly integrated, however, cannot be considered 100% reliable due to large standard deviations, poor resolution, or adverse conditions during measurements [16].

1.2.3 Impedance Electrodes

Chopstick electrodes inside a Transwell system

The use of porous membrane and what they allow (Use of porous membranes in tissue barrier), all the properties (they allow cell-cell interaction, talk about optical transparency, thin membrane)[15]

1.3 Organ-On-Chip Technology

Organ-on-chip is the technology behind the manufacture of the chip into which the membrane electrode is integrated. It is a rather recent technology, the manufacture of which is multidisciplinary in nature and encompasses several different fields of science. For this reason, to fully understand it, it is necessary to take a detailed

overview of generic microdevices, outlining the Bio-MEMS and Lab-On-Chip devices and specifying the characteristics and advantages of Microfluidic Chips.

1.3.1 Main aspects of a Microdevice

Microdevices, since their inception in the last decade of the twentieth century, have changed our view of science, due to their potential applications in fields ranging from optics, semiconductors and the microelectronics industry to drug discovery and development, point-of-care clinical diagnostics, sensitive bioanalytical systems, and other areas of the biological sphere [17] Micro-devices are available in many different types and designs, but they all share common properties that determine the ability to create these devices.

All the components present in this type of device can be grouped into three large classes. A first component of the device concerns its functionality, which directly affects the functional aspect, i.e., the role for which it is designed. A second component concerns the structural aspect, i.e., structural materials are used to both support the system and create the desired response and finally there is a third component which is the part of the sensors that allow the control of the parameters when the functional material interacts with its environment.

Despite the multitude of microsystems that can be envisioned, each can be broken down into a simple structure consisting of the active material connected to electrodes and supported by the elastic support structure [18]. Since the active material and electrodes are usually in the form of films that are not self-supporting, a very common method of producing microdevices is to build them, layer by layer, on a supporting substrate. This is the basis of many microsystems' fabrication pathways. Due of this layer-by-layer fabrication route, each subsequent material must be able to be processed within the survival window of the previously deposited materials (Figure 1.2). Each material must be resistant to the effects of heat, reactions and stresses that will be imposed during the processing of subsequent layers. This represents the main challenge for the integration of materials to produce active micro-devices[18].

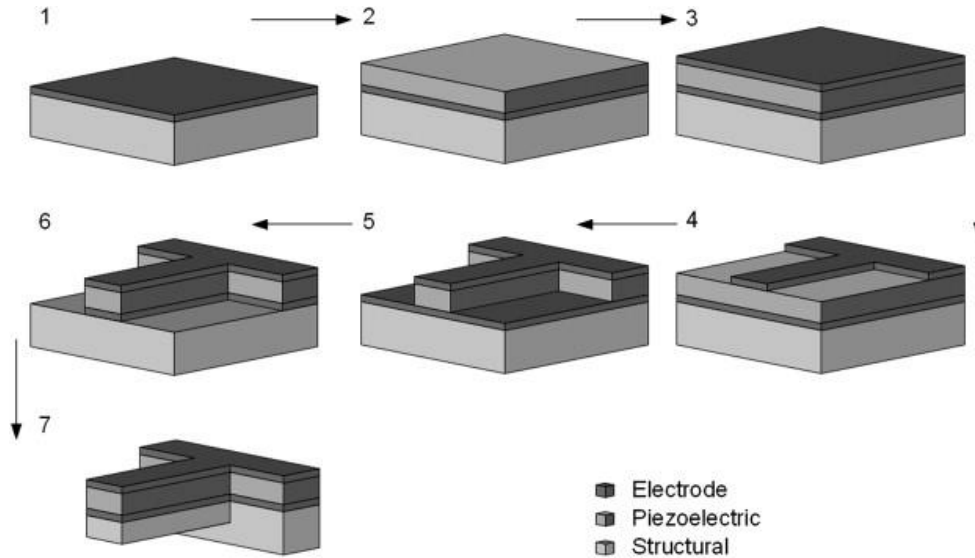


Figure 1.2: Schematic of MEMS fabrication route showing how the MEMS is built up layer by layer: 1) base electrode deposited onto substrate; 2) functional material integrated; 3) top electrode deposited; 4) top electrode patterned; 5) functional material shaped; 6) base electrode shaped; 7) substrate shaped leaving a cantilever bar.

The choice of materials and manufacturing processes is clearly linked to the ultimate purpose of the device and the functional material to be used, e.g., if the study include the necessity of working with cells, the choices that should be made during the process are completely different compared to a non-biological case.

A general classification of microdevices has been made by dividing them into three large classes according to their application (Figure 1.3). Some technologies can be considered as a hybrid between two different classes because they present aspects common to both classes, as is the case with OOC (Organ-On-Chip), which has elements common to Bio-Mems and Lab-On-Chip devices. The functionality and application of OOC technology will be discussed in more detail in the following paragraphs, but first the two classes of devices just mentioned are outlined.

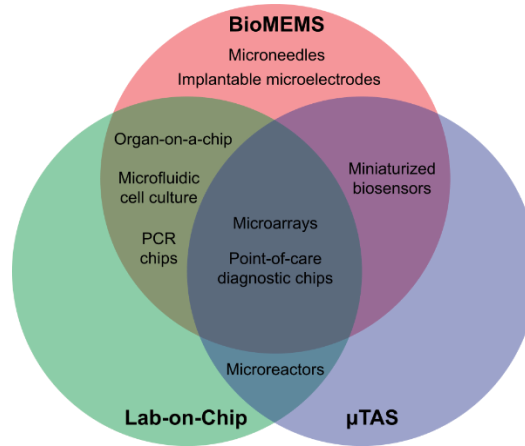


Figure 1.3: A summary classification of the microdevices.

1.3.2 MEMS and Bio-MEMS

Micro-Electro-Mechanical Systems, or MEMS, is a technology that in its most general form can be defined as miniaturized mechanical and electro-mechanical elements (i.e., devices and structures) that are made using the techniques of microfabrication. The critical physical dimensions of MEMS devices can vary from well below one micron on the lower end of the dimensional spectrum, all the way to several millimeters. Similarly, the types of MEMS devices can vary from relatively basic structures that have no moving parts, to extremely complex electromechanical systems with multiple moving parts under the control of integrated microelectronics. The label "MEMS" is used to describe both a category of micro-mechatronic devices and the processes used to manufacture them. Some MEMS do not even have mechanical parts, yet they are classified as MEMS because they miniaturize the structures used in conventional machinery, such as springs, channels, cavities, holes and membranes. The only main criterion for MEMS is that there are at least some elements that have some sort of mechanical functionality, independently of whether these elements can move or not. Whereas the functional elements of MEMS are miniaturized structures, sensors, actuators and microelectronics, the most notable (and perhaps most interesting) elements are

microsensors and microactuators. They can be appropriately categorized as 'transducers', which are defined as devices that convert energy from one form to another. In the case of microsensors, the device typically converts a measured mechanical signal into an electrical signal.

These are typically found in cars, gaming devices, smartphones and environmental testers. Many of these same MEMS are used in the medical field and are therefore called 'Bio-MEMS'[19]. For instance, pacemakers and defibrillators use some of the same sensors found in smartphones and cameras. These devices, hence, perform a medical or biological function. To give an idea of how these devices are used nowadays, the Bio-MEMS currently on the market may for example include a therapeutic system for diabetics that not only monitors glucose levels with an internal sensor but also delivers a precise amount of insulin when needed through a cannula and micro-needle inserted under the skin. Another example of a bio-MEMS that has been on the market for quite some time is the cochlear implant. The cochlear implant uses a series of electrodes implanted inside the ear to stimulate the eardrum when it receives audio vibrations from an external transmitter. Bio-MEMS, hence, is typically more focused on mechanical parts and microfabrication technologies made suitable for biological applications, the fields of application of this technology are many and endless possibilities.

1.3.3 Lab-On-Chip and Microfluidics Devices

Specifically, Lab-On-Chip (LOC) refers to devices that miniaturize and integrate laboratory processes and experiments on a single chip [19]. It is a miniaturized device that integrates into a single integrated circuit, commonly called chip, one or several analyses, which are usually done in a laboratory: analyses such as DNA sequencing or for instance biochemical detection. The chip can be from a few millimeters to a few square centimeters to achieve automation and high-throughput screening [20]. Research on lab-on-a-chip focuses on several applications including human diagnostics, DNA analysis and, to a lesser extent, the synthesis of chemicals [21].

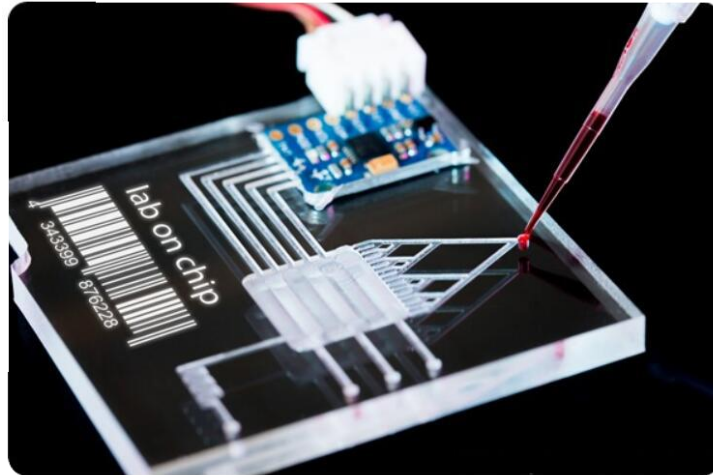


Figure 1.4: *Conducting an analysis in a Lab-On-Chip device*

Lab-on-a-chip devices are a subset of microelectromechanical systems (MEMS) devices and sometimes called "micro total analysis systems" (μ TAS). LOCs can use microfluidics, physics, manipulation and the examination of extremely small quantities of fluids. However, in a narrow sense 'lab-on-a-chip' generally refers to the scaling up of single or multiple laboratory processes to chip format, whereas ' μ TAS' is concerned with the integration of the total sequence of laboratory processes to perform chemical analysis. The term 'lab-on-a-chip' was introduced when it was discovered that μ TAS technologies were applicable to more than just analysis (Figure 1.3). The emergence of this field mainly relies on two core technologies: microfluidics and molecular biology. Microfluidic technologies used in lab-on-a-chip devices allow millions of microchannels, on the order of a few micrometers, to be fabricated on the chip. Microchannels allow the manipulation of fluids in quantities of a few picolitres and the processing of biochemical reactions in very small volumes. In order to enable all these operations, lab-on-a-chip devices are not only a collection of microchannels, but they also require the use of integrated pumps, electrodes, valves, electric fields and electronics to become complete lab-on-a-chip diagnostic systems [21].

1.3.4 Organ-On-Chip Devices

Articles: Smart Device, One stop Microfluidics solution

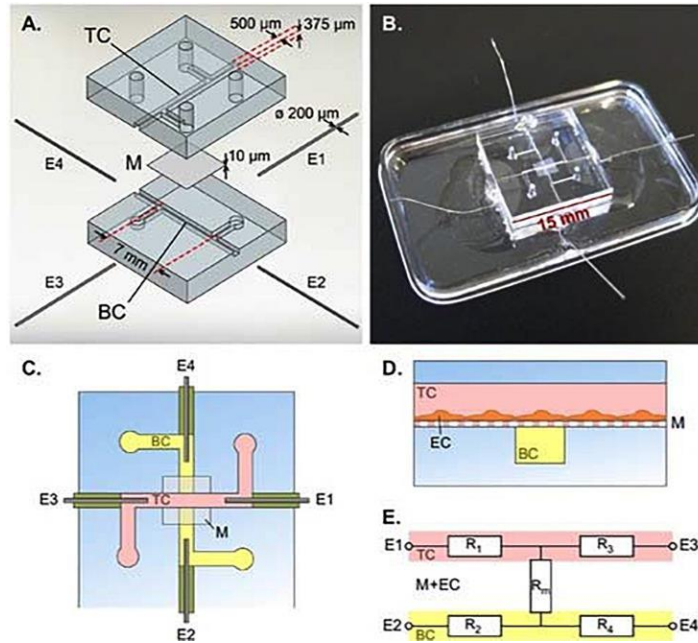
Why we use microfluidics devices, what are the news in this topic, property of the microscale, what we can do that we cannot do with other devices

Nowadays, in vitro models that mimic the in vivo behavior of an organ like OOC device or a whole being (human-on-chip) device are becoming increasingly popular. These models, using human cells, reproduce specific functions of the human body in order to conduct experiments and at the same time, from an ethical point of view, they also allow to drastically reduce the exploitation of animals in the laboratory representing a valid and a also more accurate alternative to the use of animals.

1.4 Barrier-on-chip model device

In this section we will go into why the use of a chip is so important in constructing a barrier model and what are the advantages of placing membrane electrodes directly within a chip device.

Highlight benefit of barrier-on-chip device compared to others barrier device,

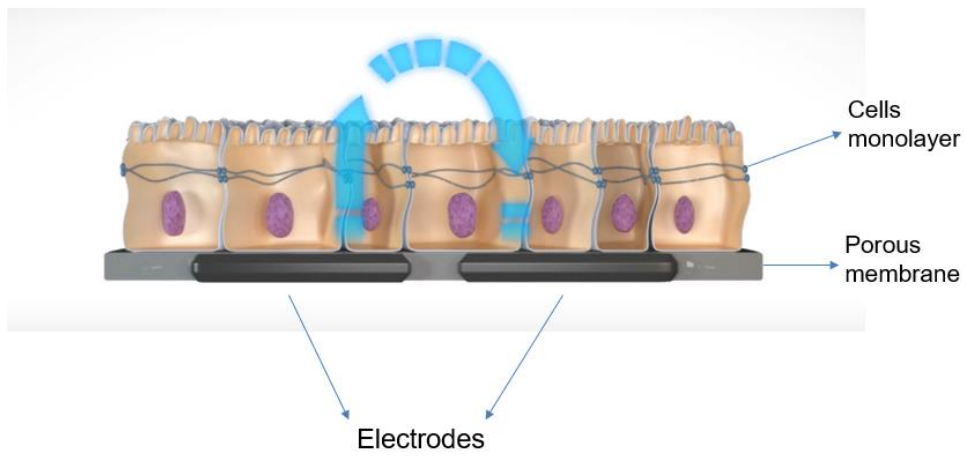


[22]

1.4.2 On chip sensors integration

Chopstick electrodes inside a Transwell system

The use of porous membrane and what they allow (Use of porous membranes in tissue barrier), all the properties (they allow cell-cell interaction, talk about optical transparency, thin membrane)[15]



Membrane embedded electrodes allow direct integration during assembly of the chip

Talk about the Integration of impedance electrode in barrier model device for real time measurements,

Materials and Methods

Methods

2.1. Chip Design

The chip used in the project was designed using CAD (*Computer-aided design*) software (*Fusion360 from Autodesk®*). The device in question was designed to mimic the behaviour of a human body barrier in vitro. A dual-chamber chip was therefore structured to simulate two different compartments, which were then separated by a central cell culture layer consisting of a track-etched PET (Polyethylene Terephthalate) microporous membrane [23], [24]. The use of 12 µm thick membrane with 0.4µm pores (*lot number:M/220119/R/3, it4ip®*) enables to mimic the exchange of nutrients that takes place in vivo between two different compartments thanks to their pores that allow certain substances to pass through[25], [26]. PET membranes are extremely transparent, an important property for cell profiling via microscopy to eliminate background [27]and they are furthermore very thin, which provides better interaction between the two compartments, closer to the in-vivo system, as well as enhanced diffusive and hydraulic permeability[28] . Both the basal and apical compartments were designed to be used as fluidic channels and accordingly include inlet/outlet to be perfused with culture media, creating a liquid-liquid interface between them[29]. The inlets and outlets were suitably positioned to promote easy handling and perfusion of the channels. Both compartments therefore have the same geometry and feature a central circular-shaped area with a diameter and size equal to that of a 96-Well plate to ensure that cell culture can be promoted[30]. The only difference between the two compartments may concern the height of the chambers in the development of the device, which was specially designed to be modular to allow for an interchangeable and adaptable design for the various possible barrier-on-chip (BoC) models and the microporosity of the membrane can also be chosen differently depending on the type of barrier to be mimicked [31]. In the chip in question, since

it was intended to validate the model by means of gut cells modelling a Gut-on-chip(GOC) barrier, it was decided to set a basal compartment height of 0.5 mm, as literature has shown that this is the ideal height for HUVECs endothelial cells that need some stress during perfusion to properly develop [32], [33], whereas a top channel height of 1 mm has been found to be ideal for CACO-2 epithelial cells[34], [35]. It can therefore be employed for simple cultures but can also be a suitable model for cell co-cultures[36], [37]. Both sides of the membrane middle layer can be exploited and different media cultures can also be used. Within the two compartments, the use of four small pillars was also conceived and designed, whose primary purpose is to help support the central layer that will later house a cell culture within it, and secondly, thanks to their shape, they also help the fluid distribution within the chamber[38]. The use of supports in this design allows the cells to be sustained in a stable plane, which is crucial for high-throughput screening assays[39], [40]. The design was conceived to support both a static culture and a possible dynamic culture through a peristaltic flow, for instance [41].

In the following sections, different manufacturing techniques for the BoC in question will be explained in detail, analyzing their benefits and drawbacks defining the final manufacturing method chosen.

Figure of the chip

2.2. Chip Fabrication

2.2.1 Layer-by-Layer Chip

The device was firstly designed with a computer-aided design (CAD) software (AutoCAD from Autodesk®). The first fabrication method that was tried involved the construction of the layer-by-layer chip using a bottom-up technique. The layers are composed of Polydimethylsiloxane (PDMS) sheets, a silicon-based elastomer, bonded on top of each other[42]. The different layers were fabricated through Xurography, a rapid prototyping technique that requires the use of a cutting plotter machine (Roland Cutters) which was guided through Roland CutStudio®, software that enable precise cut [43]. In this setup, the design of the chip was imported as a simple JPG into the software, in which some of the cutting parameters (*Cutting*

force = 80 gf, cutting speed cm/sec, Blade offset = 0,50mm) were directly cut through the 0,5mm thick PDMS sheets using a blade, thus obtaining the various layers. The design of the chip in object was obtained by drawing a device with the external dimensions of a 75cm x 25cm rectangle, the size of a laboratory glass slide that allows the chip to be easily handled and involved in all laboratory processes, inside of which four equally sized chambers were inserted (figure 2.2).

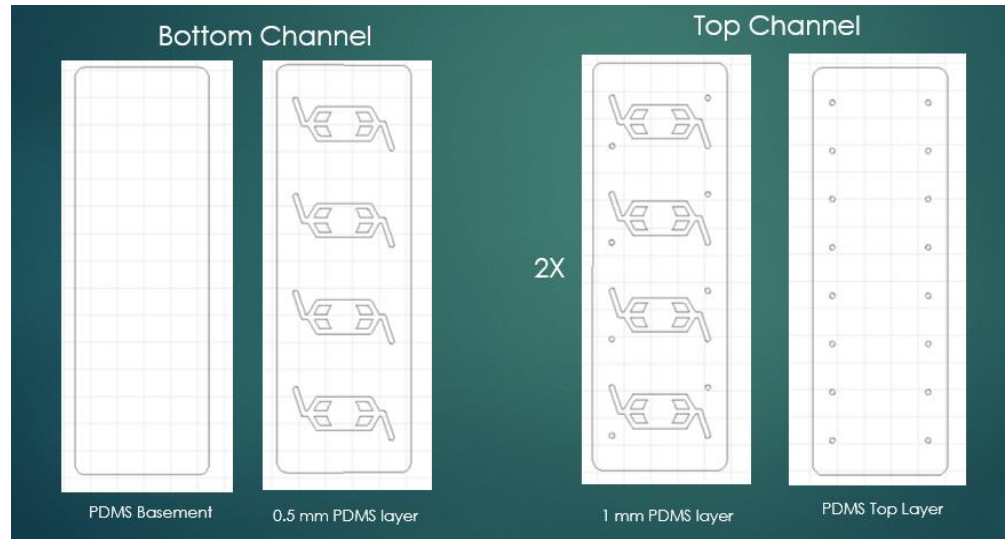


Figure 2.2: The figure shows the different PDMS layers used in producing the final chip. On the left side are images of the parts for the Bottom Channel, the other two on the right were used to build the Top Channel. Since 0.5mm PDMS sheets were used, two layers were bonded to construct the upper compartment of 1mm.

The assembly of the various layers that were cut was achieved through Oxygen plasma treatment (300 W; 0.7 Torr; 120s)[44]. The different PDMS layers were subjected to a 2 min plasma treatment that activated the exposed surface, making PDMS-PDMS bonding of the various layers possible[45]. It's important to wipe with a tissue soaked with Isopropanol the plasma chamber before use it. Both pieces to be bound, after being plasma activated, are manually aligned one on top of the other and placed in an oven at 80 °C to rest for an hour in order to seal the bonding [46].

The resulting workpiece can then be used to eventually bind another layer on top, proceeding again as described above.

2.2.2 PDMS-Casting Chip

Considering the inefficiency of the previous method, a process was attempted that would allow for fast manufacturing times while at the same time not requiring manual alignment of the pillars, which makes the fabrication method non-reproducible. The option of creating molds from the CAD drawing of the chip was therefore considered[47]. The idea was to fabricate the molds and use them to cast the PDMS prepolymer inside with the 10:1 curing agent (Sylgard 184) to make PDMS casting[48] and simply obtain the various layers without having to build the chip layer-by-layer by manually aligning the various layers[49], [50]. The use of a cloud-based 3D modeling software platform (*Fusion 360 from AutoDesk®*) was required to have a 3D drawing of the Master Mold. After that, we tried to figure out the best manufacturing method to obtain molds that were high resolution to avoid losing the geometry of the chip and at the same time with a smooth surface in order not to have rough surfaces that could affect the transparency of the chip, which is very relevant for optical analysis [39], [40]. Starting from the same chip drawing, two different models were extruded to make two different molds for the bottom and top channels respectively. The 3D models once finished were exported as .STL file from Fusion360. These models will then be used to generate our casting molds, and depending on the manufacturing technique chosen, they can be made of different materials. First molds were made using a resin and through a **process of ????**. However, these molds have shown not to have perfectly smooth surfaces. Various methods were attempted to try and smoothen the surfaces of the molds by testing various acetone baths in different concentrations but without achieving total smoothness. Consequently, it was decided to maintain the method as it was efficient in terms of layer results but changing the material and mold manufacture to have transparent layers. The new master has been custom manufactured by a company(*imaterialize.com*), starting from exported .STL file from Fusion360, through Selective Laser Sintering (SLS) in which the monomers are sintered by laser to obtain the final 3D model. Two molds, one for the bottom layer and one for the

top layer, were used as masters to obtain the two pieces of the chip. After having the master molds, the PDMS chip parts are easily obtained by simple casting of a PDMS-prepolymer (solution 10:1 of PDMS-prepolymer and the curing agent) in the molds. For this passage, 10ml of the solution, using Sylgard 184 kit as explained before, is prepared. To avoid the formation of bubbles, the solution is degassed using a vacuum chamber[51] for about 20min until the bubbles have almost all disappeared or are on the surface and simply by blowing on them or pricking them with a needle they can be removed[52]. Approximately 6 ml is then poured into the master mold relative to the top layer, which has greater height and thus greater depth in the mold, and approximately 4 ml into the bottom layer. The molds are then placed on a flat surface and any bubbles formed during casting are eventually popped. Lastly, a protective foil is applied to the two molds in order to level the prepolymer throughout the layer to achieve a flat surface and well-distributed component (figure 2.5).



Figure 2.5: *In the figure, the molds used for the top layer (left) and bottom layer (right) respectively. A protective plastic foil was then applied to both of them to facilitate even distribution of the mixture.*

This will then help to have a perfect bond in the next step, ensuring that the two layers can adhere at all points without any problems. The molds can then be placed in the oven at 70°, allowing the mixture to harden quickly (in about two hours), or if the molds are sensitive to high temperatures, they can be left over night at room temperature as an alternative in order not to damage them[52].

2.2.3 Final bonding of the whole chip

Once the top and bottom layers are fabricated, the final bonding of the two pieces with the PET membrane in the middle of the chambers has to be carried out. A method was pursued to effectively seal the chip so that it could later be exposed to a possible long cell culture[53]. The bonding is carried out through a glue solution. A silicon prepolymer elastomeric base (*Sylgard™ 184 elastomeric kit*) is mixed in the ration 1:10 with the curing agent from the same kit, this solution is then mixed with Toluene, an organic solvent, in the ratio 60:40 to obtain a viscous glue solution[54]. In this method, the elastomeric base is used as a mortar and allows leakage-free bonding [55]. The glue is then set aside for 15 minutes to allow the solvent to evaporate slightly, and in the meantime, glass slides are appropriately cleaned, which will be used for the spin coating operation. Laboratory glass slides are cleaned using an ultrasonic cleaner. The glass slides are immersed in a specific liquid alkaline concentrate for highly effective cleaning (Hellmanex III® 2% in water) and sonicated for 5 minutes. This is followed by another 5 minutes of sonication with isopropanol and finally another 5 minutes in water[56], [57]. The cleaned glass slide is then quickly dried through an air gun and left in an oven at 80° for 5 minutes. Once dry, 1.5 ml of the previously pre-prepared solution is spread over the glass slide, which is then evenly distributed over the surface using a spin coater. The slide is spun for 30sec at a speed of 800rpm. A thin layer of glue is now evenly distributed over the glass slide. The final assembly consists of impregnating the bottom layer onto the slide glass, transferring a thin layer of glue onto the workpiece. Subsequently, only the extremities of purposely cut rectangles of PET membrane are impregnated to cover the entire chamber. It should be mentioned that it is important to avoid transferring glue to the middle part of the membranes [54]. as

this could block the pores of the membranes, causing them to lose their intrinsic microporosity property. This process requires some manual handling and the use of tweezers to transfer and place the membranes correctly is strongly recommended. Once the membranes are positioned on the bottom layer, the soaking process is repeated for the top layer, which is aligned above the bottom layer, sealing the chip. The system is then transferred to an oven at 120°C and left overnight to ensure a leak-free and perfectly sealed system[45], [53].

2.3. Chip Validation

In this section follows a careful description of the validation processes that were carried out to ensure that the chip is leak-free, that dynamic culture can be performed, that it can hold medium inside for long periods to handle cell cultures, and that it provides a good environment to house the cells.

2.3.1 Ink validation assay

The first test that was performed inside the chip concerns validation by ink. The aim was to optically evaluate that the two compartments divided by the PET membrane were truly sealed and independent, that the membrane had no cracks and that there were no spots where the two sides could exchange fluids other than through micropores. To this purpose, the two chambers were filled with inks of different colors, red for the upper chamber and blue for the lower chamber, to assess that on the inlet and on the outlet the colors remained the same to be sure that the two compartments did not interchange their respective fluids. Pure ink is mixed 10% in water for both colors and the chambers are then loaded through a pipette.

2.3.2 Flow analysis assay

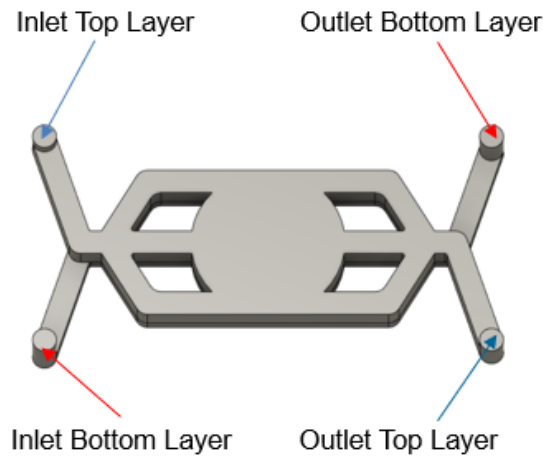
Green fluorescence beads (Fluoro-Max™, diam. 4.8 μm, *ThermoScientific*) were used to validate the flow within the chip and ensure that the entire surface of the chamber was filled properly and that the particles were able to flow seamlessly and without getting stuck inside the chip. To perform these analyses a glass slide was applied above the chip through an oxygen plasma treatment (300 W; 0.7 Torr; 120s). Via the same method explained above, it is in fact also possible to bind PDMS

and glass[58]. The glass slide is properly drilled to have holes at the inlets and outlets of the various chambers to ensure that the flow is not obstructed. The application of a glass layer is important to promote adhesion of the ports that are used to allow connection with the peristaltic pump tubing to promote fluid circulation within the chip under dynamic conditions. The application of ports above the glass layer is done using an epoxy glue (*EA 9492, Henkel*). Using a needle, the glue is distributed around the individual port, which is sliced from microfluidic tubes (Tygon LMT-55, ID: 0,51mm) to a height of about 0.4cm. The ports are then positioned at the holes on the glass slide to match the inlets and outlets of the chambers and dried in an oven at 70° for about 20 minutes[59]. The chip is then perfused thanks to the use of the pump of a solution of fluorescence microspheres (Fluoro-Max™, diam. 4.8 μm, *ThermoScientific*) 1:100 diluted in H₂O. Then, by means of employing a fluorescence microscope (Cell Vivo Life Cells Microscope, *Olympus Life Science*), some videos were recorded which were then later analyzed using TrackMate a tool performing tracking, data visualization, editing results and track analysis distributed in FIJI which is an image processing package based on ImageJ2.

2.3.3 CFD Validation

Finally, computer-based fluid dynamic analyses, in particular using CFD (Computational Fluid Dynamics) software from Autodesk®, were also performed. It enables analysis of fluid flows using numerical solution methods[60]. In this case, Autodesk's CFD software was used. Starting again from the chip drawing, a 3D model was constructed by extruding the inner part of the chamber this time, aiming to create a 3D model representing the entire volume occupied by the fluid flowing in the chambers (Figure 2.9). The model was then imported to the software where the main parameters and the boundary conditions were set as the materials used[61]. In detail, the middle layer was specified as a PET membrane while the top layer and bottom layer, i.e., where the fluid actually flows, was identified as a liquid material corresponding to a certain viscosity, water or PBS (Phosphate buffered

solution) in this case. Importing the middle layer into the model is important and makes it clear that the two chambers are physically separated and that there is no direct contact between the two flows of the top and bottom compartments. Next, flow-related parameters such as flow rate or various inlets/outlets were then specified. The latter are identified by the software as air-liquid interface points by being set as points having a pressure equal to atmospheric pressure.



By finally setting the various fluid threads and thus declaring how the fluid actually flows, the simulation starts, leading to different kinds of analysis. These analyses detect the areas of highest flow pressure, enabling to understand if the cells are possibly under excessive stress, and they are also important to visually comprehend if there is a direct perfusion in the whole chip or if there are areas that remain uncovered or where the fluid gets stuck.

2.4 Cell culture

A validation of the chip was also performed to see if it could really accommodate medium- to long-term cell culture. It was aimed to check whether the cells could grow inside in a proper way and become confluent without being damaged during culture[62], [63]. At the same time, it was also sought to see if the chip could accommodate a cell culture for a long time without having medium leakage[53]. To

this end, a cell culture of CACO-2 was performed in several chips as a proof-of-concept. Caco-2 is an immortalized cell line of human colorectal adenocarcinoma cells. It is primarily used as a model of the intestinal epithelial barrier[64]. Among its most advantageous properties is its capacity to spontaneously differentiate into a monolayer of cells with several characteristics typical of the absorptive enterocytes with brush border layer found in the small intestine[65], [66]. The Caco-2 cell line is heterogeneous and contains cells with slightly different properties. It was seen that even as the various cell passages varied, some relative properties, such as the TEER measurement tended to increase as the passage increased[67]. In the chip in question, the aim was to create a monolayer of intestinal cells in the upper compartment of the chip and understand how they behave during cell culture. In the next sections, first some functional arrangements that were made to the chip to house the cells will be presented, and then how the cell culture was carried out and once the various chips were seeded, what kind of analysis were performed.

2.4.1 Chip preparation for cell culture

To prepare the chips for cell culture, starting from the structure already described, some features were added to create a welcoming environment for cells. First of all, reservoirs were made from a solid layer of PDMS obtained following the previously described method using PDMS prepolymer and curing agent. This time instead of pouring the mixture into molds and letting it harden, about 30ml are poured inside a small petri dish. Then using a razor blade, small cubes of PDMS are obtained, which are then punched out using a biopsy punch with a diameter of 4mm. These then undergo the usual plasma treatment along with the already assembled chip to make sure that they can then bond. The exposed side of the reservoirs are then aligned at the various inlets and outlets of the chip. The use of the reservoirs within the cell culture is of essential importance since not only it creates a liquid-liquid interface that extremely facilitates the change of medium and allows for no bubbles within the chip, but it has also the function of providing an extra amount of medium to the chip preventing therefore the medium inside from drying out. PDMS in fact, allows gas permeation[68], which makes it a beneficial feature as it allows the chip to exchange gases with the incubator environment but at the same time it is very

easy for the medium inside to dry out causing cell death. Another very important feature when it comes to cell culture inside a chip is collagen coating. Having a collagen coating above the PET membrane promotes cell adhesion because it recreates an ECM (extra-cellular matrix)-like environment and thus a system that closely resembles that in vivo[69]. The chips, however, before undergoing collagen coating are sterilized externally through Isopropanol, then they are also sterilized internally by filling the chambers with 70 % Ethanol, and finally they are placed in a petri dish and left in the incubator overnight. The next day, after washing the compartments with PBS to remove any traces of ethanol, Type I collagen coating is applied to the upper compartment, which is the one in which a monolayer of cells is to be recreated. The coating is performed under a laminar flow hood, filling the upper compartment of the chip for its entire volume (about 100 μ l) with 5% Type I collagen (*Sigma*[®] – *Life Science*) solution in PBS (*Sigma*[®] – *Life Science*). The chip is then left in an incubator for about 1 hr. After this period, the chambers are washed again with PBS, and at this stage they are ready to house the cells.

2.4.2 Cell Expansion and seeding in the chips

For all cell-related processes, all steps were performed in a laboratory wearing lab coat always, putting on gloves and taking care that all sterile operations were performed under a class II laminar flow hood. All materials or instruments used under the hood were specially sterilized before introduction into the cabinet. There is an initial process in which CACO-2 cells are in principle expanded by standard 2D culture in T75Flask. The cells are cultured in an incubator at 37.5°C, 5% CO₂ and 21% O₂. When the cells are confluent (about 90%), the other procedures are continued with the ultimate goal of seeding the cells inside the chips in which collagen coating was previously done. As a first step, the medium is aspirated with a aspiration pipette connected to a suction system. Next, the flask is rinsed at least twice with PBS being careful not to place the liquid directly on the wall where the cells are still attached. This process is to ensure that effectively all the medium is aspirated. The next step involves the insertion of trypsin, which is used to cause the cells to detach; this occurs because trypsin is an endopeptidase, which digests proteins. In the trypsinization process extracellular proteins are digested, which

leads to the detachment of the cells from the bottom of the culture vessel. The presence of residual medium therefore, more specifically the presence of serum that contains protease inhibitors could inhibit trypsin. Therefore, 3ml of Trypsin is added and carefully spread over the entire surface. The system is placed back in the incubator for about 5min after which it is taken out and gently tapped on the walls so that all the cells detach. A look under the microscope is then taken to make sure that the cells are floating. 5ml of medium is then added to precisely inhibit trypsin, the prolonged use of which could damage the cells. After this, the solution is gently mixed with a pipette to make sure that all the cells are really collected of and that no clumps are formed. The total amount is then transferred to a 15ml falcon tube. The cells are then centrifuged for 5min at 170rcf in a laboratory centrifuge in order to drive them to settle to the bottom of the falcon tube. The solution of medium and trypsin is then aspirated very carefully and then 6ml of fresh medium is added and the cells are resuspended inside the falcon tube by gently pipetting. At this stage, the cells are counted to subsequently seed the chips with a desired number of cells. A sample of about 10ul is taken from the resuspended cell solution, and the number of cells is determined with a hemocytometer, which is a counting-chamber device. Using this device, the cell density can be derived by means of the following equation:

$$\text{cell density [cells/mL]} = \text{number of total amount of cells} / \text{number of large viable squares cells} * 10,000 * \text{dilution factor}$$

Different densities (0.5M cells/ml, 1M cells/ml and 1.5 cells/ml) were calculated and different chips with different cell concentrations were tried in the course of experiments, but it was seen that seeding the chips with a density of 1M of cells/ml is a good factor to have enough cells to form a monolayer inside the chip (whose chamber volume is about 100 μ l). The chips are then seeded at a density of 1 million cells per ml. The medium is easily changed daily by the presence of reservoirs that facilitate replacement, and throughout the period of the experiment the chips are always placed inside the incubator. To facilitate a total medium replacement, it is usually attempted to aspirate with a micropipette for 1/3 of the chamber volume from the outlet reservoir, while reintroducing fresh medium from the inlet reservoir

again for 1/3 of the total capacity. The operation is repeated 5/6 times to allow for total medium turnover. This allows the reservoirs to never be completely emptied by maintaining a minimum liquid level that always permits a liquid-liquid interface. This will make it much easier to avoid trapping bubbles inside the chip during the medium changeover.

A culture is therefore performed inside the chip for a maximum period of 7 days to perform some analyses on the viability and morphological arrangement of the cells, which will be described in the next sections.

2.4.3 Live/Dead Staining

During cell culture within the chip, live/death staining is performed to verify the viability of the cells, particularly at day 3 and day 7 of the experiments. To determine the viability, staining solutions were prepared freshly. On day 3, it was decided to evaluate the viability of some device chambers. Considering that the total chamber volume is about 100 μl a total solution of 1ml in PBS was prepared in these proportions: Calcein (0.5 $\mu\text{l}/\text{ml}$), Ethidium Bromide (2 $\mu\text{l}/\text{ml}$). Within metabolically active cells, AM(Acetomethyl) calcein is converted by cytosolic esterases to green, fluorescent calcein. Fluorescent calcein is held by living cells with intact membranes. Hence, it is only cells possessing active cytosolic esterases that turn green. This makes it possible to quickly and easily identify metabolically active (viable) cells in a sample. Its excitation (ex) and emission (em) wavelengths are 495 and 515 nm[70]. In contrast, ethidium bromide cannot penetrate inside metabolically active cells, so it cannot interact with DNA, staining instead only dead cells with permeable cell membranes. In this case the fluorescence compounds will exhibit an excitation peak of 301 nm and an emission peak of 603 nm[71]. At this stage that the solution is prepared, chambers were filled using twice the volume needed to fill a chamber by the usual method across reservoirs to ensure that no traces of medium were left behind and to allow the fluorescent compounds to act in a proper manner. These operations were performed under a hood in the dark to avoid photobleaching of the compounds. The device is incubated at 37.5 °C for 30 min. The chambers are then rinsed with PBS before performing viability analysis with a fluorescence microscope to then acquire images. Images are acquired by

having a Z-stack. Through ImageJ software, the images are overlaid by reconstructing the best frame.

A further viability assay is performed on day 7 by repeating the exact same steps listed above. The only difference from day 3 is that an additional dye is added to support the presence of an extra control. In fact, fresh staining solution is prepared following the previous compounds and concentrations but adding in this case Hoechst in 10 $\mu\text{l/ml}$ concentration. It can pass through the cell membrane, intercalating with DNA and therefore is able to make all cell nuclei fluorescent (ex 361 nm, em 486 nm). This makes further controls possible through software such as ImageJ since, for example, by exploiting only the signals at the emission wavelengths of Ethidium Bromide and Hoechst and then counting through ImageJ the cells, by subtraction of the dead cell signal to the signal related to Hoechst it is possible to estimate as a percentage the live cells i.e., those corresponding to the signal of Calcein.

2.4.4 ICC Assay - Tight junctions Staining

A tight junction (TJ) assay is also performed on day seven. This allows verification that a monolayer of cells has formed within the chip and that cell-cell connections are promoted. In fact, epithelial and endothelial cells are connected by a set of intercellular junctions that regulate diffusion between cells and permit endothelia and epithelia to form cellular barriers that separate compartments of different composition. These intercellular ports formed by the tight junctions are not only being highly regulated, but are size- and ion-selective and, hence, provide a semipermeable diffusion barrier[72].

The tight junction assay is an Immunocytochemistry (ICC) assay that can confirm the expression and localization of target protein peptides or antigens in the cell through a specific combination of antibodies and target molecules. These linked antibodies can then be detected by a variety of methods. In general ICC allows scientists to evaluate whether or not cells in a specific sample express the antigen in question. In this specific case, it was intended to evaluate the presence of Zonula occludent-1 (ZO-1) using an indirect detection fluorescent assay. ZO-1 is a high

molecular mass phosphoprotein that is encoded by the TJP1 gene in humans and is a TJ-associated protein. The protocol described below for ZO-1 staining was followed. Since this is a very long procedure, it was performed on two different days. First, the cells at day 7 of culture inside the chip are removed from the incubator. The first step concerns cell fixation, it is done using 4% Paraformaldehyde (PFA) in PBS for 10min at room temperature (RT). Then the chamber should be subjected to 3 washes with PBS lasting 5min each. After this step, the device can be stored at 4°C as the cells are fixed awaiting staining or the next steps can be performed immediately. At this stage the cells must be permeabilized and this is done with 0.1% v/v Triton X-100 for 15 min at RT. This is followed by three more washes with PBS of 5 min each. The chip is then incubated for 1 h with the blocking solution which is composed of 10% GOAT serum in PBS. Meanwhile, primary antibodies are prepared and diluted in 1% goat serum solution in PBS. For this step we need antibodies specific for ZO-1, which is precisely our target, in our case ZO-1 Rabbit PolyAb (56 ug/150ul) was chosen. The chip is then incubated in the refrigerator in the dark for 12-14h overnight, and then the rest of the procedure is carried on the following day. The day after, the process begins again with 3 more washes of the chambers with PBS for 5 minutes each. The solution with the secondary antibodies is prepared at this time. They have a conjugated fluorescent molecule and are responsible for binding to the FC region of the primary antibodies. Since the primary antibodies prepared in a rabbit were used, it is necessary to choose secondary antibodies compatible to the primaries used. Alexa Fluor 488 goat anti-rabbit (1:200) were employed in this experiment. The system is incubated 1h at RT after insertion of the secondary antibodies. It is important that all steps from now on are done in the dark so as not to damage the fluorescence (photobleaching) of the secondary antibodies. It is continued with 3 more washes in PBS of 5 min each. A counter-staining is then carried out by incubating the chip with Hoechst 33342 solution (1:1000; 1 µg/mL in PBS) for 10 min, RT. Finally, the process was ended by performing 3 more washes of the chambers with PBS of 5 minutes each. Lastly, the images were acquired using a fluorescent microscope and then processed with ImageJ.

2.5. Electrodes Fabrication Method

The protocol described here is an adapted and optimized version of the protocol [73]. It is a bi-layer photolithography process leading to high-resolution microporous membrane-based gold electrodes. The procedure involves the use of standard PET membranes (pore size = 0.4 μm ; thickness = 12 μm , ipCELLCULTURE™ Track Etched POLYESTER - Product Reference: *lot:220119/R/3, it4ip®*). By this process, gold electrodes can be deposited on porous membranes achieving a resolution of 2.5 μm . However, it can also be used to structure other metals (e.g., copper, chromium, titanium) or combinations thereof. It is therefore possible to ensure high resolution in reproducing electrodes despite their fabrication on a very thin and flexible substrate like a microporous PET membrane. The steps of the protocol are clearly outlined in the figure below (*figure 2.10*). It begins first by standard washing protocol with 2% (v/v) Hellmanex solution, isopropanol, and deionized water (diH₂O) of the glass slides. PET membranes should also be cleaned in this case to be sure there is no residue. The membranes are soaked first in diH₂O (15min) and then in Isopropanol (15min). Then, the membranes are dried in a hot plate at 120°. The glass substrates are then treated with O₂ plasma (300 W; 0.7 Torr; 45s) to facilitate the diffusion of the PVA glue layer. In fact, to adhere the membrane to the glass substrate, PVA glue diluted in diH₂O (40 mg/ml) stored at RT is employed. To prepare this solution, it is important to dissolve 4 g of PVA in 100 mL of diH₂O and stir the solution at 70°C until the PVA is completely dissolved. During this process, it is advisable to cover the container with aluminum foil to prevent water evaporation and then filter the resulting solution using a syringe filter (22 μm). For spin coating, it is necessary to place a thin piece of PDMS (larger than the slide) on the spin coater support and then transfer the plasma-treated slide to the top.

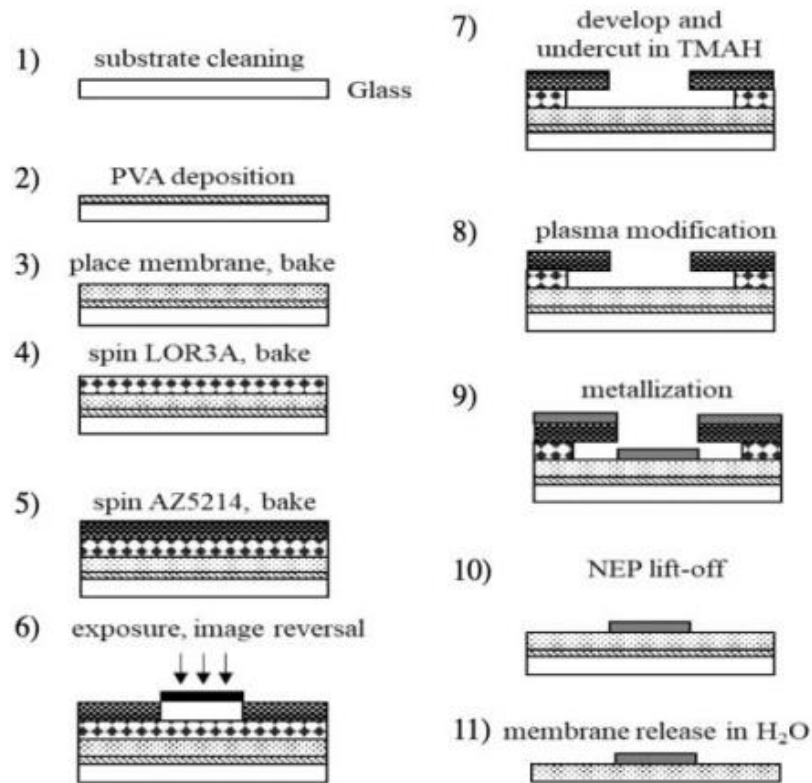


Figure 2.10: Electrodes fabrication protocol. The image represents all the steps of the electrode fabrication process. It begins with the membrane and slide cleaning processes (1), continues with PVA deposition (2), membrane bonding (3), then follows the application of the two layers of photoresist (4-5), a double UV exposure one with mask and one without (6), development in a special solution that dissolves the Photoresists in the part not exposed to UV light(7), i.e. the part covered by the mask. This is followed by an argon plasma treatment (8) that allows the gold to adhere to the substrate during sputtering (9), and finally, steps (10) and (11) depict the two final steps of removing excess gold and the final detachment of the membrane from the slide in water.

This will help create the vacuum despite the slide being smaller in size than the spin coater. And then around 1.5mL of PVA solution is spread on top of the glass slide (with a Pasteur pipette). Parameters 30s and 800 rpm (Revolutions per minute) are then set as input, and the spin coater is started. It is important now to have a lot of

manual dexterity because after the slide is spun, the thin layer of glue that has been evenly deposited on top dries very quickly, so it is important to quickly place the membrane on top to glue it in place. This is the most delicate step in the entire protocol, and it is very important that the membranes be folded slightly before being placed to avoid the formation of bubbles or wrinkles. With gentle pressure therefore, the membranes are placed in the center of the slide and are immediately baked at increasing temperature. It is in fact important that the slide is completely dry at the end of the process, but at the same time, it is not desired to dry the system all in a rush to avoid causing the presence of bubbles, so the membranes are slowly dried by ramping the temperature every 3 minutes until it is brought to 150°C. First 3 minutes are carried out at 70°C, then 3 minutes at 100°C, followed by 3 minutes at 120°C and finally 3 minutes at 150°C. If the samples are baked too fast, the evaporating water will cause wrinkles on the membrane. Once dry, the protruding ends of the membranes from the slide are then cut off with a cutter. This process turns out to be even easier if the glass slides are still slightly warm. Once this step is performed, the membranes can then be stored in a petri dish or the protocol can be continued immediately with photoresist deposition. Therefore, two layers of two different photoresists are deposited. The layers are deposited through a spin coater. The principle that is being followed is to use two negative photoresists and a negative mask. A negative resist means that it is soluble in the specific solvent if untreated. The photoresists are stored in the refrigerator at 14°C. To collect them from the vial, 10ml syringes are employed. They make the process faster and more precise and allow the resist to be deposited on the slide that is placed on the spin coater just as in the case of glue application. It is required to first apply the first photoresist and then let the deposited layer dry. Roughly 1.5 ml of LOR3A is poured onto the slide, which is then spin-coated at 1000 rpm for 30s. A soft-bake process of 180s at 150°C ensues. At this stage, as the first layer is adhered on the substrate, the deposition of the second photoresist is then performed. AZ5214E is poured through the syringe onto the spin coater and pinned at 3000 rpm for 30s. It is succeeded by soft bake process for 60s at 100°C. It is achieved as an overall result a glass slide with the integrated membrane having the two layers produced by the two photoresists on top of it. This is followed by a process of exposure to UV (365nm)

light, this allows the parts exposed to the light to reticulate while keeping the parts covered by the mask unreticulated and thus soluble. An initial exposure of 4s at 100% power is made. The sample is at this point baked at 120°C for 70s to stabilize the structure, followed by subsequent exposure to UV light without mask which is carried out for 5s at 100% power. At this point the photoresists result to be cross-linked in the parts exposed to UV light. This makes these parts non-removable once the sample is developed. The development is performed in AZ726MIF for 60s which is a Tetramethylammonium hydroxide (TMAH) based developer. Then the slide is rinsed thoroughly in water, being careful not to remove the membrane since PVA is water soluble. At this stage, the shape of the electrodes has been imprinted on the membrane, the sample is then ready to undergo a sputtering process. An Argon plasma treatment is first carried out inside the sputtering chamber. This activates the parts of the membrane not having the resists and modifies their surface in order to then accommodate the sputtered gold more effectively. The sputtering process is in fact a phenomenon in which a solid material, in this case gold, is ejected from its surface, after the material is itself bombarded by energetic particles of a plasma or gas. In this process, 80nm of gold is deposited through a sputtering system on top of the whole glass slide. The sputtering process takes place at an internal chamber pressure around 2×10^{-4} mbar, at a current of 100 mA. Since the sputtering rate of the machine is about 1.05nm/s, for each electrode it was set the total sputtering time to 110s including 30s of pre-sputtering to verify that the material is actually etched properly and 80s of effective sputtering above our sample. The last step that follows is lift-off. The purpose of this process is to remove the gold from the entire slide by having it remain only within the electrode shape meaning the unexposed part of the mask, those that specifically do not contain the resist. In fact, the lift-off in this case consists of a bath in a solution to remove the resist and thus the non-patterned gold. It is performed in a glass petri dish where N-methyl pyrrolidone is poured in. The solution is shaken with a lab shaker and the sample deposited inside through tweezers. Rotation of the lab shaker coupled with the use of a pasteur pipette helps to remove excess gold. From time to time, to aid removal, the same compound is sprayed with high pressure through a syringe above the electrodes to remove any remaining gold fragments attached. Finally, only the last step remains i.e., removing

the membrane from the glass slide, which is easily carried out by immersing the sample in diH2O. The final product is a membrane upon which 3 high-resolution thin-film gold electrodes have been fabricated.

2.6. Electrodes Validation

Once the electrodes have been fabricated, a validation part of the electrodes then follows. It is indeed necessary to investigate the performance of the electrodes, the reliability of the same, and thus provide a proof-of-concept. To do this type of evaluation, several different solutions were attempted. Initially, it was tried to validate the electrodes directly and straight away their fabrication. In each case, validation involves the use of a potentiostat in order to be capable of performing impedance measurements. The potentiostat is electronic hardware that is used to conduct electroanalytical experiments. Externally it appears as a large box from which we have several available channels each working independently. For each channel in a basic configuration there is a three-electrode system[74].

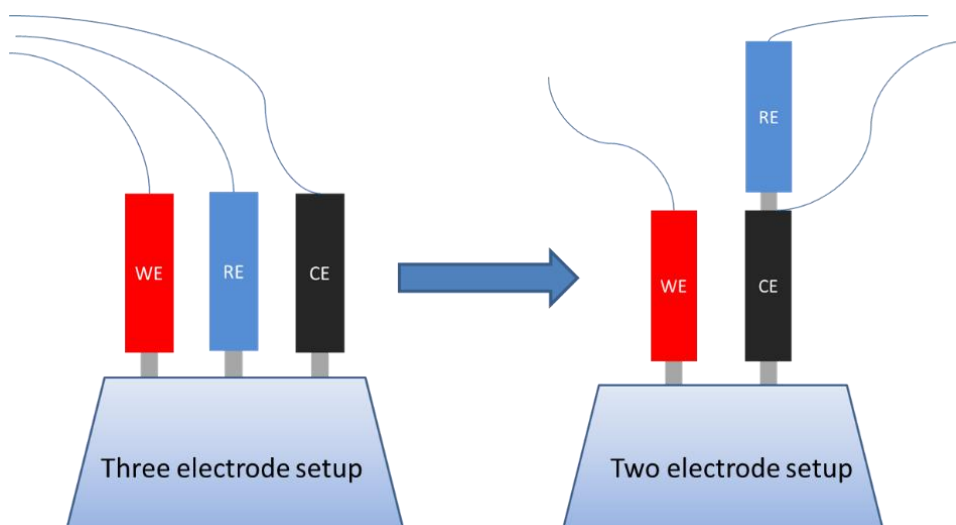


Figure 2.14: The configuration on the left represents the classic three-electrode setup. The one on the right represent the configuration for this experiment that is a two-electrode setup since the final goal is to connect the two ending of the potentiostat to the contact pads of the interdigitated electrode to perform impedance measurement[75].

In the three-electrode setup there are three electrodes in use namely the working electrode (WE), the reference electrode (RE) and finally the counter electrode (CE). The extremities of the electrodes are then, through connectors, plugged into the device to be tested, thus closing the circuit. In the three-electrode setup there are three electrodes in use namely the working electrode (WE), the reference electrode (RE) and finally the counter electrode (CE). The extremities of the electrodes are then, through connectors, plugged into the device to be tested, thus closing the circuit. In the current case, it was chosen to perform measurements using a two-electrode setup in which the RE is short-circuited and the CE also acts as a reference (figure 2.14). There are therefore only two free ends that need to be connected to the contact pads of the interdigitated manufactured electrode to be able to perform measurements.

2.6.1 Impedance with crocodile clips connectors

In a first system the electrode is chosen to be placed directly on a glass slide, crocodile clips are selected as possible connections. In the current case, conductive copper tape is also used to attach the membrane to the glass slide to enable the crocodile clips to have a conductor-conductor interface when they are directly hooked to the glass slide (*figure 2.15*). A variable frequency voltage is then applied in order to induce a current and thus measure an impedance. The values chosen in the potentiostat parameters are the reference values for typical impedance measurements (Voltage: -10V:10V, Frequency: 100mHz:100KHz). In this setup to perform the impedance measurements, once all connections were made, a drop of an electrolyte solution (ferri/ferrocyanide solution) was deposited over the interdigitated part of the electrode by means of a micropipette.

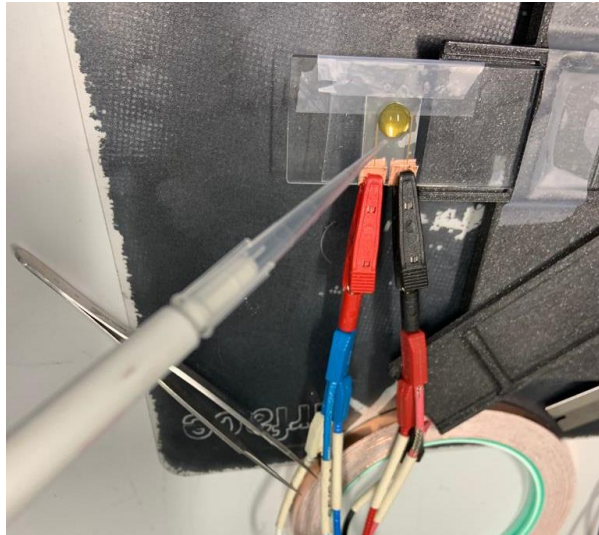


Figure 2.15: The picture shows the configuration with which measurements were performed.

Through a micropipette, a drop of the electrolyte solution is released above the interdigitated electrode. The crocodile clips are hooked to the glass slide directly over the copper tape that allows the connection between the electrode connector pads and the crocodile clips themselves.

The problem with this arrangement is related mainly to the fact that the drop is constantly being deposited and propagated in different ways. This affects the reproducibility of the measured impedances, which were indeed found to have widely divergent values; therefore, stability in repeating a measurement in the same condition to a previous one could not be guaranteed. For this purpose, it was considered to integrate the electrodes inside a chip for more detailed assessment. A very simple device design consisting of a single dual-chamber chip, intended to validate the electrodes and to recreate the environment of a barrier-on-chip, is realized through Xurography. The various layers of the chip, after being cut from a PDMS foil are then bonded together after being treated with plasma oxygen that activates them. We therefore obtain, as in the previous case, a bottom and a top chamber. The membrane, which has the electrode that is to be evaluated, is then utilized as the middle layer. The final bonding is also carried out again by making the glue used previously i.e., elastomeric prepolymer 1:10 with curing agent (60%) and toluene 40%. The procedure used to obtain the chip is the same, the glue is

spread evenly on a big glass slide (800 rpm, 30s) through a spin-coater, the surface of the bottom layer is dipped in the glue, then it is proceeded by soaking in the glue the limbs of the membrane which is then placed on top of the bottom layer and finally the top layer is also soaked in the glue. Finally, aligning the 3 layers, the device was obtained (*figure 2.16*).

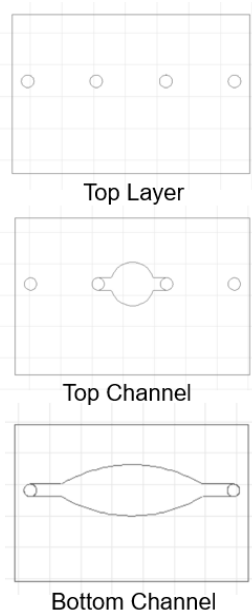


Figure 2.16: *The figure on the left shows the main layers that were then produced through the cutting plotter and with which the chip shown on the right was then fabricated, showing the final integration of the electrode inside the chip. It can be observed that the middle layer composed of the membrane is intentionally protruding to permit connections with the crocodile clips.*

The chip is then placed under pressure using clips and left 3h to achieve a tight seal in a 120°C oven. A PDMS holder is then fabricated that is hooked to the rest of the chip using conductive copper tape, which in addition to anchoring the chip has a double function since it is used to allow the connection between the membrane electrode pads and the crocodile clips of the potentiostat (*figure 2.17*).

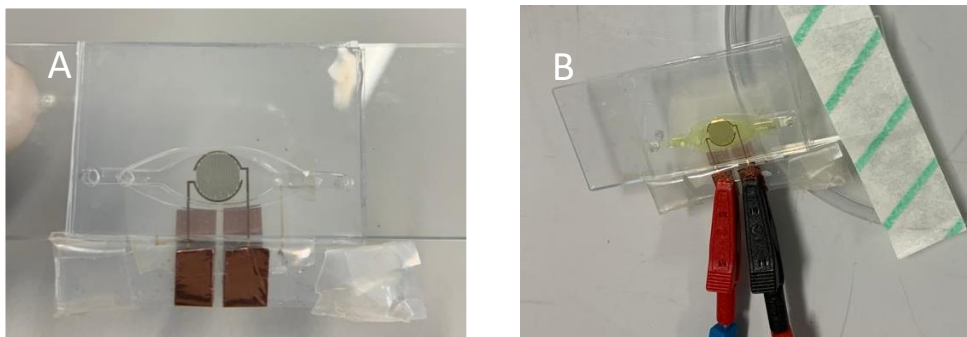


Figure 2.17: A) It can be observed the chip with the PDMS support integration hooked by means of the copper tape. This facilitates the connection with the crocodile clips afterwards. B) In the figure, the chip is fixed and then connected to the potentiostat with the crocodile clips.

Measurements made in this system with the potentiostat, appear to become much more reliable, and also highly reproducible. The electrolyte solution was directly inserted inside the top layer allowing the central surface of the electrode to be fully covered in the interdigitated part. The volume occupied by the electrolyte solution was kept constant by the use of the chip, which made the measurements coherent. However, a difficulty was denoted in using direct connections since the copper tape did not adhere well to the electrode pads or since they are very sensitive it sometimes ruined them, stripping some of the gold part of the pads and making any further connections impossible. Some help was given using a silver paint that once applied to the edges of the electrode-copper tape interface assisted in some cases to close the loop and thus promote a current flow inside, however in these cases, since the connections were made substantially all in a different way, it resulted in impedance shifts in the real part, which will be discussed in the results section subsequently.

2.6.2 Impedance with pogo pins connectors

It was therefore considered to change the type of connectors, for the purpose of having a more stable system that would not cause the typical shift in the real impedance part that is due to a different connection to the circuit each time. The goal is therefore to have connectors that connect the electrodes to the potentiostat in exactly the same way, so it was decided to change the chip design slightly. Previously the electrode pads were prominent to allow connection through the

crocodile clips, now the entire membrane including the pads are integrated within the chip. It was planned to use pogo pins, which by their structure, allow a connection from the top. The top layer is then designed so that the pogo pins can access the chip in correspondence of the connector pads of the membrane electrodes. Substantially, the top layer is cut with a cutter blade so that it can be accessed from above the chamber. To enable the pogo pins to then be anchored in such a way that they would remain fixed during measurements, a custom holder is printed through a 3D printer using fusion360 software. The holder in question, houses the pogo pins and keeps them in place immobile and once the connectors are placed in position above the pads, it is itself attached to the chip through clips (figure 2.18).

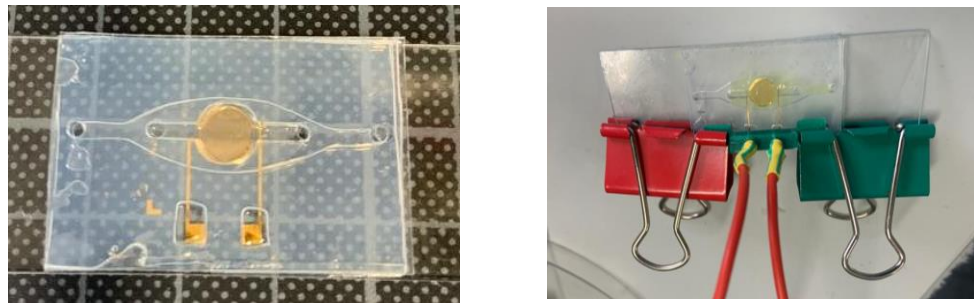


Figure 2.18: The left picture displays the new fabricated chip with the appropriate adaptations. The membrane is no longer protruding from the chip, and the top layer has been punched out so that the pogo pins can be accessed from above. The pogo pins are embedded inside the green 3D substrate that was purposely printed with a 3D printer. The holder is then fixed through clips to the glass slide on which the chip is fabricated.

In this type of setup, it is much easier to conduct measurements. Once the chip is positioned as in Figure 2.18, the top layer is filled with the electrolyte solution. In this case, the problem of the previous shift of the real part of the impedance is not recorded, as everything is fixed properly here, guaranteeing a circuit with connections identical to themselves even after days and different measurements.

2.6.3 TEER in presence and absence of compounds

Since a stable setup was found, it was decided to provide a proof of concept of the electrodes by validating them with CACO-2 cells and verifying that the electrodes were able to measure the TEER of the cells. The goal is to prove that once a cell monolayer has actually been formed above the membrane electrodes, the TEER increases dramatically, hence detecting a severe increase in impedance. Next, it was wanted to verify that a barrier disruption was also detected by our electrodes, so a nonsteroidal anti-inflammatory drug (NSAID), more specifically diclofenac, was added to the chip to assess that it really did decrease barrier impedance. In fact, it has been found in the literature that this type of drug makes intestinal cells leaky, causing disruption of the barrier[76], [77]. Reservoirs are then added above the chips, which will help throughout the cell culture process. On day 1, an impedance measurement of the electrodes is performed. The chip chamber is filled with the CACO-2 cell culture medium and the preliminary measurements are performed initially without cells. These measurements will then be compared with those taken after a 3-day cell culture. To the chips, collagen coating is applied and they are left in the incubator for about 1h. This, as previously seen, helps the cells to adhere. Next, the chips are seeded with CACO-2 cells with a concentration of 1 million cells per ml. Cell culture takes place as described in the previous case, and at day three it is decided to effectively measure the TEER of the cells. The chips are removed from the incubator, the medium is exchanged so that it is fresh, and chips are connected via pogo pins to the Potentiostat. Since it is intended to keep the chips sterile, as they are then to be incubated overnight again in order to conduct further measurements, PCR tape is used to block all inlets and outlets above the reservoirs. Measurements are then carried out with the Potentiostat. A chip in which no cells were seeded was used as a control measurement. Then a solution containing diclofenac is prepared and applied to the different chips. Two 50mg tablets are first rubbed against the sandpaper to remove the external coating and subsequently pulverized through a mortar. Next, a solution of diclofenac in PBS is prepared. It goes through the calculation of the number of moles (mol), known the molecular weight(g/mol) and mass(g) in grams of the compounds, and thereafter, having fixed the molarity $M(\text{mol/l})$, that in our case is $200\ \mu\text{M}$, the amount of PBS in ml to be

added to the compounds is calculated to reach the solution with the desired molarity. The prepared stock of compound must then be diluted to have a molarity comparable to those seen in the literature (2000 μM /1000 μM)[76]. Therefore, from the initial stock prepared having a molarity of 200 μM , the compound is then diluted within the culture medium at a ratio of 1:10. The chips are incubated with the medium with diclofenac overnight and then the results are analyzed by TEER measurement the following day.

List of Materials

List of Chemicals (WE SHOULD SEPARATE THE MATERIALS THEN)

Materials	Manufacturer
Antibiotics	Sigma Aldrich
AZ5214E	?????
Biopsy puncher	Stiefel
Cell culture flasks 75 cm^2	Greiner BioOne
Cell tracker	Thermo Fisher Scientific™
Cutting Plotter	Roland
CellVivo Life cell microscope	Olympus Life Sciences
Centrifuge	Eppendorf
Collagen I	Sigma – Life Science
Diclofenac genericon	Genericon Pharma
DMEM (Dulbecco's Modified Eagle's Medium) high glucose	Gibco
Epoxy Glue	Henkel
Ethanol 70%	VWR Chemicals
Extrusion Printer	Prusa®
Falcon Tube 15ml, 50ml	Greiner BioOne
FCS (Fetal calf serum)	Thermo Scientific™
FBS (Fetal bovine serum)	Thermo Scientific™

Fluorescence microspheres Fluoro-Max™	Thermo Scientific™
Goat Serum	?????
Hellmanex III®	Helma Analytics
Incubator	Eppendorf
Isopropanol	VRW chemicals
Laminar-flow hood	Thermo Electron
LOR3A	?????
MEM (Minimum Essential Medium)	Gibco
Microscope IX71	Olympus Life Sciences
Microscope glass slide	VWR
N-methyl pyrrolidone	?????
Non-Essential Amino Acid (NEAA)	Gibco
Pasteur pipette	Greiner Bio-One
PBS (Phosphate buffered solution)	<u>Sigma – Life Science</u>
PET (Polyethylene terephthalate) membrane ipCELLCULTURE™	It4ip®
PDMS (Polydimethylsiloxane) sheets	MVQ Silicones
PFA (Paraformaldehyde)	<u>????</u>

PVA (Poly (vinyl alcohol))	<u>????</u>
Petri dish	Greiner Bio-One
Pipette tips	Ep. T.I.P.S.
Pipettor	SARSTEDT
Prusament PLA Green	Prusa®
Silicon elastomer base	SYLGARD 184
Silicon curing agent	SYLGARD 184
Silver paint	<u>????</u>
Toluene	<u>????</u>
Trypan Blue	Fluka
Trypsin	Sigma Aldrich
Triton X-100	<u>????</u>
Tygon Tubing	ISMATEC®
Water Bath	Grant Instruments
ZO-1 Rabbit PolyAb	Proteintech®

Media Culture (2 types)

Table for Instruments in the lab

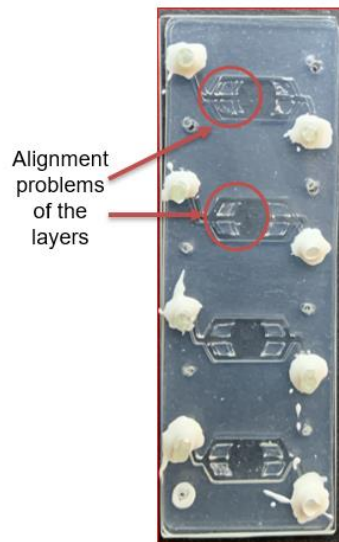
3

Results and Discussion

3.1 Results

3.1.1 Alignment in the layer-by-layer chip

This fabrication method was discarded as fabrication required the use of 5 total layers (2 for the bottom channel and 3 for the top channel). The manual alignment of the various layers complicated the process especially in the part of the pillars for the membranes, which made the method not really reproducible as well as very expensive both economically and in terms of time (figure 2.3).



3 **Figure 2.3:** *the figure shows the result of the bottom-up layer-by-layer chip. The main problem that makes the method not reproducible is the manual alignment of all 5 layers used. This makes the method time-consuming and difficult to reproduce.*

3.1.2 Smoothness of the molds

First molds were made using a resin and through a **process of ????**. However, these molds have shown not to have perfectly smooth surfaces (figure 2.4). Various methods were attempted to try and smoothen the surfaces of the molds by testing various acetone baths in different concentrations[78], [79]

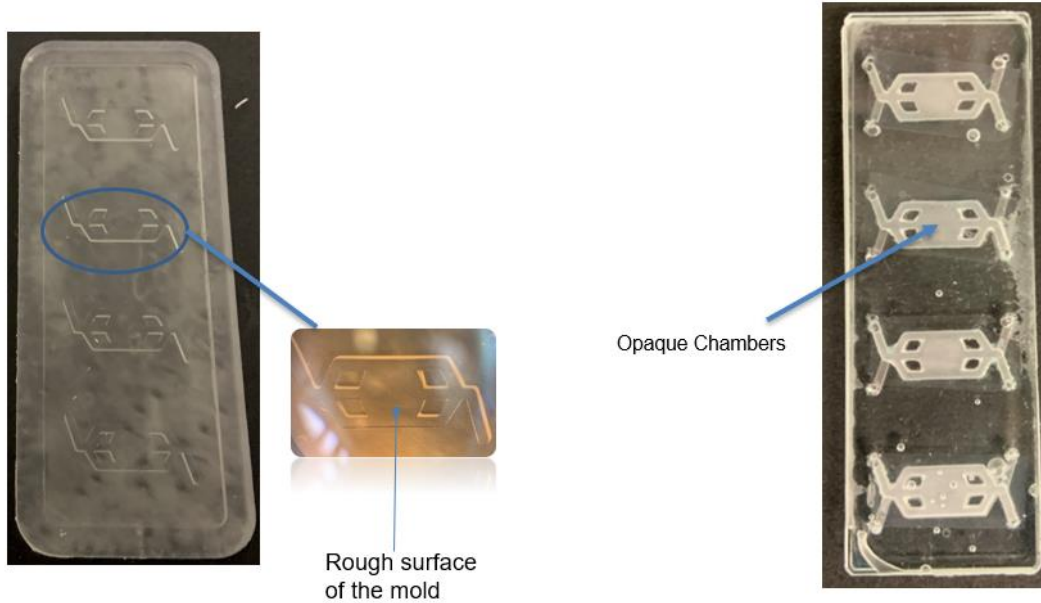
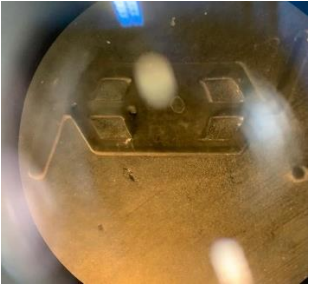
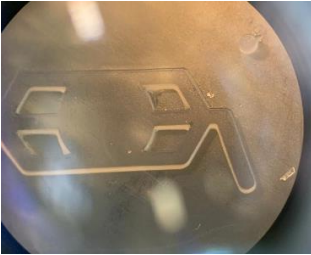
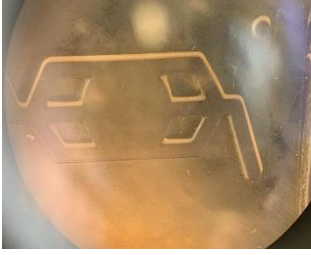


Figure 2.4: the figure shows on the result of the fabricated white resin mold. As can be seen, the surface is rough. This leads to problems in casting the various PDMS layers, which are consequently opaque and not transparent as can be observe on the chip figure on the right.

The following table summarizes the various attempts made by varying the parameters of acetone bath time and bath concentration:

Timing	Acetone Concentration	Result
No treatment	No treatment	
5 min	10% in H ₂ O	
5 min	20% in H ₂ O	

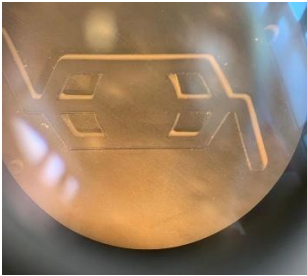
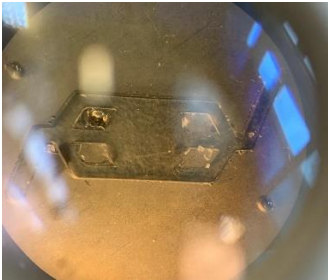
10 min	20% in H ₂ O	
20 min	20% in H ₂ O	
5 min	30% in H ₂ O	

Table 2.1: *The table presents a detailed follow-up of the smoothing operation of the manufactured molds. It divides the various attempts according to the exposure time of the acetone bath carried out in an ultrasonic cleaner to agitate the molecules faster and the various concentrations used for the bath.*

The various experiments have certainly improved the surface of the molds by making it smoother, however, it has not been possible to treat the structure to have a fully smooth surface. In fact, the castings tried on these molds have resulted in

cloudy, opaque, rough-surfaced, and not perfectly transparent layers. Overexposure to even higher parameters such as those of 30% acetone treatments have in fact only ruined the structure without bringing any noticeable improvement (Table 2.1). Consequently, it was decided to maintain the method as it was efficient in terms of layer results but changing the material and mold manufacture to have transparent layers. This fabrication method was discarded as fabrication required the use of 5 total.

3.1.3 Final chip by PDMS casting

The result of the final bonding and the chip obtained is illustrated in figure 2.6. Subsequently, certain analyses are conducted on the chip to ensure that there are no leaks, that the flow distribution inside is regular and that the chip can be used for cell culture.



Figure 2.6: *Illustrated is the fully assembled device. It consists of 4 bicameral chips, each of which has 4 inlet/outlet chips appropriately staggered to fill/change the medium or culturing cells. It can be*

noticed that the chip is completely transparent even inside the chambers, allowing good optical feedback during cell culture.

3.1.4 Sealing evaluation by Ink

A comparison of the output color with the input color is carried out optically (*figure 2.7*). Talk about the chambers and how they dont mix colors



Figure 2.7 *Validation assay using reddish ink for the top layer and a bluish for the bottom one. The figure shows the real independence and absence of direct communication between the two compartments since the fluid colors at the chip inlet are the same as those at the outlet. The only way the two layers exchange fluids is by means of the micropores in the track-etched PET membrane, which mimics the behaviour of an in vitro barrier.*

3.1.5 Flow analysis evaluation

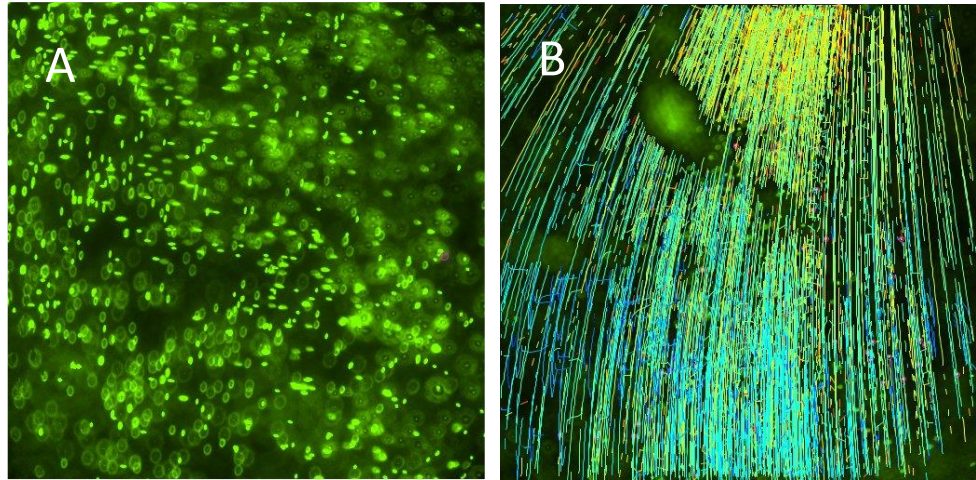


Figure 2.8 A) A frame of one of the videos recorded during the perfusion of fluoresce beads. B) One of the final images extracted by ImageJ by overlaying the various frames of the same video and tracing the particle paths inside the chip.

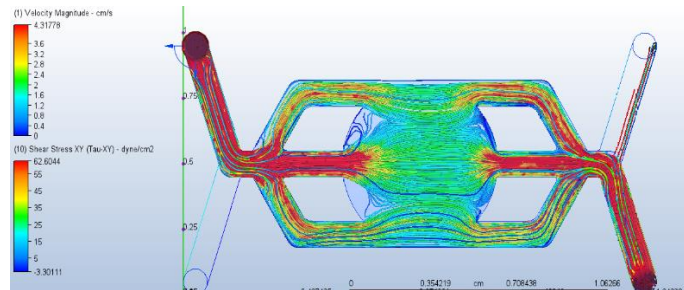
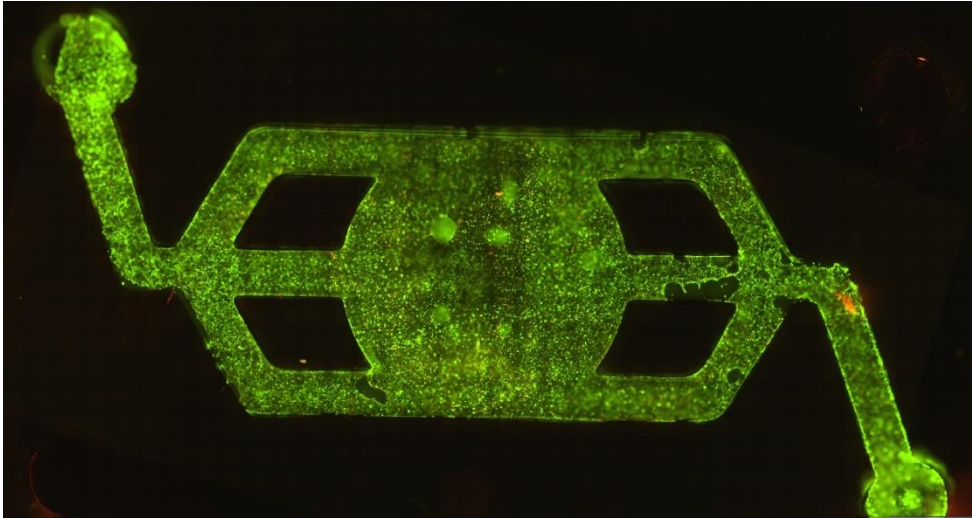
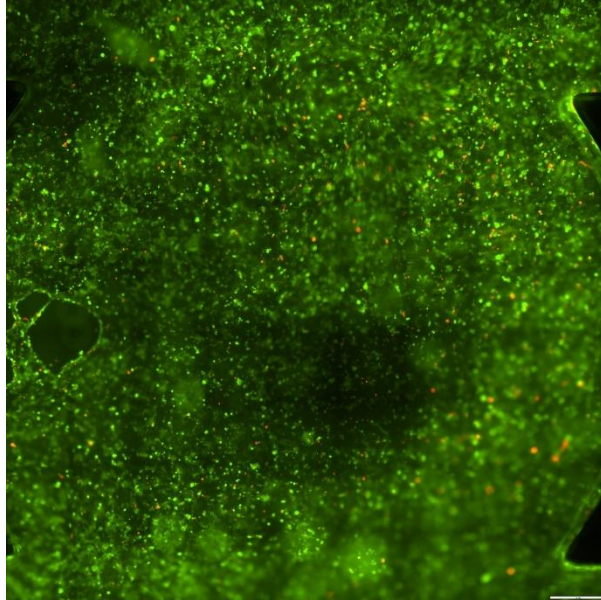


Figure 2.9 The figure above represents the 3D CAD model from which we started to do this type of analysis. It represents the volume occupied by the fluid during flow. The bottom model, on the other hand, represents one of the CFD-type analyses performed. Specifically, it can be seen how the parts subjected to the greatest pressure and therefore potentially to the greatest stress are those related to inlet and outlet, where precisely no cell cultures are expected so the cells are not at risk of stress due to the flow.

Thanks to these simulations it's possible to identify the areas of highest pressure of the flow, to understand if the cells are possibly under excessive stress, and the second is to understand if there is direct perfusion of the whole chip or if there are areas that remain uncovered or where the fluid gets stuck (figure 2.9)[60].

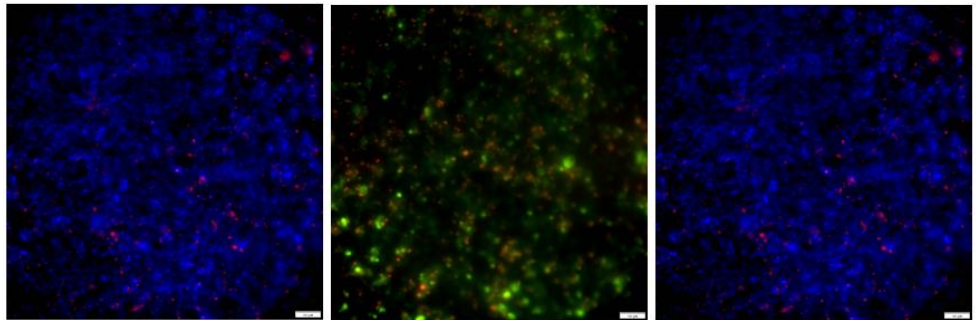
3.1.6 Cell culture results



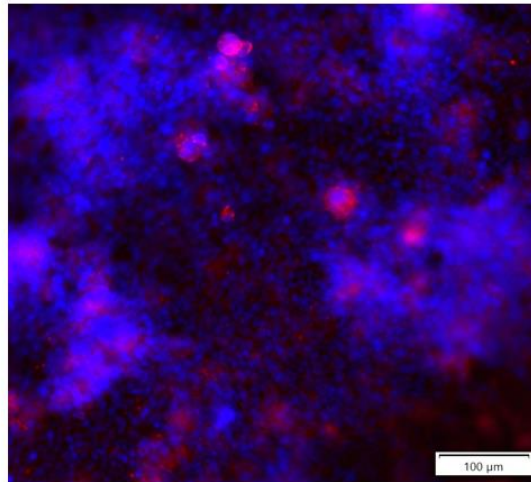
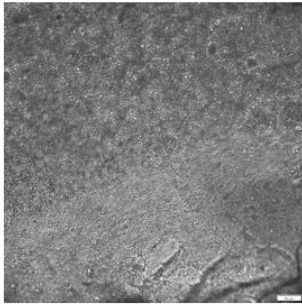
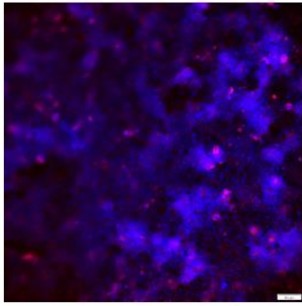


Live Dead Assay on Day7:

- Hoechst ($10 \mu\text{l/ml}$)
- Calcein ($0.5 \mu\text{l/ml}$)
- Ethidium Bromide ($2 \mu\text{l/ml}$)



**Tight Junction Assay on Day7:
Indirect detection fluorescent ICC**



ADD DESCRIPTIONS AND COMMENT!

3.1.7 Electrodes Protocol Optimization

In this section, it was highlighted in detail what were the most critical parts of the protocol to be managed and adapted to the available equipment. In particular, the most obvious critical aspects of the process were described and discussed in detail, the optimization of which led to a final protocol with high reproducibility. Finally, a different method compared to the protocol [73] is also proposed for the lift-off of excess gold after sputtering and which resulted in a higher final yield in terms of electrode fabrication.

Parameters that affect the result:

1) Oxygen Plasma Treatment:

The oxygen plasma treatment of the glass slide is a very crucial passage. A slide undergoes plasma treatment (300 W; 0.7 Torr; 45 s) to prepare the surface for the glue. In this way, it can be distributed it evenly. It has been observed that avoiding this treatment does not allow the glue to distribute throughout the slide and a long plasma exposure instead causes too many bubbles at the time of gluing the membrane.

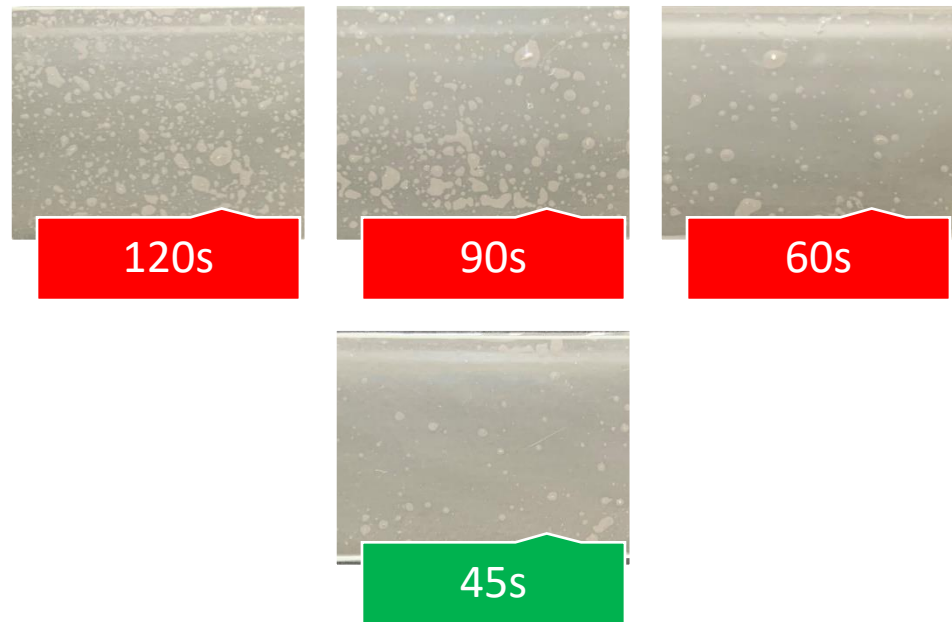


Figure 2.10: Oxygen-Plasma Treatment pre-gluing. The images are of the membrane glued to the slide which has undergone plasma treatments at different times. The longer the time, the more the bubbles increase in number and generally decrease in size. A minimum treatment of 30 seconds is still required to spread the glue evenly. At 45s, even if some bubbles are still present, the glue is perfectly distributed evenly and the bubbles present are small and oriented towards the sides of the membrane, which does not affect the success of the process in the least.

If there are too many bubbles on the surface, the result is compromised because the image impressed by UV light may not irradiate uniformly the whole slice, at the bubble for instance the photoresist may not adhere properly to the surface or when the slide is inserted into the development solution, some bubbles may break off, compromising its adhesion of the membrane or affecting the entire shape of the

electrodes. Overall, these factors lead to a loss of resolution. However, it is important in the process to position the mask so that the bubbles are at the electrodes so as to avoid the problems during UV exposures.



Figure 2.11: The figure shows two cases in which bubbles affect the final result. In the first case, small bubbles lead to losses of resolution at different points and scattered especially in the central part of the electrodes. In the second case, large bubbles leading to large localized losses in certain parts of the electrode. Both cases represent a problem, the electrodes cannot be considered ready for the sputtering phase. The defects in both cases are not visible a priori but only once the slide is placed in the development solution.

2) UV light Exposure

As described earlier, there are two main exposures that occur during the process. The second UV exposure, the one without the mask, is perhaps the key step in the final success of the protocol. At this stage it is very important to maintain a certain UV light exposure time. The purpose of this is to strengthen the image, but overexposure to UV light can cause cross-linking of the photoresist in the areas previously covered by the mask, i.e., the areas where the electrode shape is present. The aim is to keep these areas uncross-linked so that the photoresists can be solubilized in an organic solvent.



Figure 2.12: In the two figures above, the UV exposure time is too long, which has led to cross-linking even in the areas of the electrode itself and thus to a loss of final shape. Particularly in the case of exposure for 25s, there is near cross-linking of the left electrode. In the figure at the top right, i.e., the 15s exposure, we can still see that the dose was too high, the electrodes are barely visible and we have obtained the opposite effect to that desired. The last case of 5s is instead the best one. The structure is quite robust, even without the sputtering phase the shape of the electrode is clear, defined and clearly visible.

3) Lift-off process

The liftoff process is the most delicate process in the entire protocol. After the gold sputtering phase, the excess gold layer must be removed. The aim is to induce the detachment of the gold in the areas where the resists are still attached[80].

By using a solvent, the resist layers are induced to detach and since the gold layer is sputtered on top of the whole glass slide, it is consequently possible to remove the exceeding gold as well. The gold stratum will then only remain in the desired region of the electrodes. While a lift-off method based on the use of an ultrasonic cleaner was proposed in the fabrication protocol, in which the samples were sonicated at low power, it was seen that as efficient as this method was in some cases when the power set in the instrument was really very low, in others it turned out to damage the entire device.

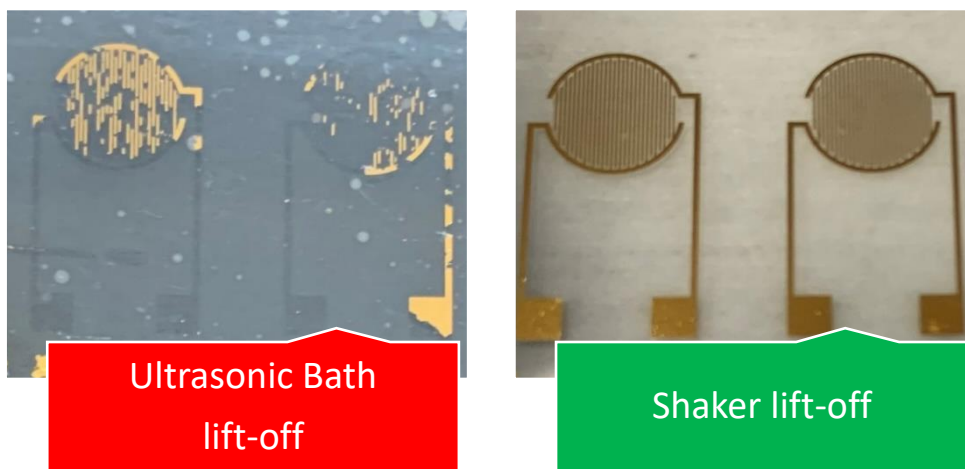
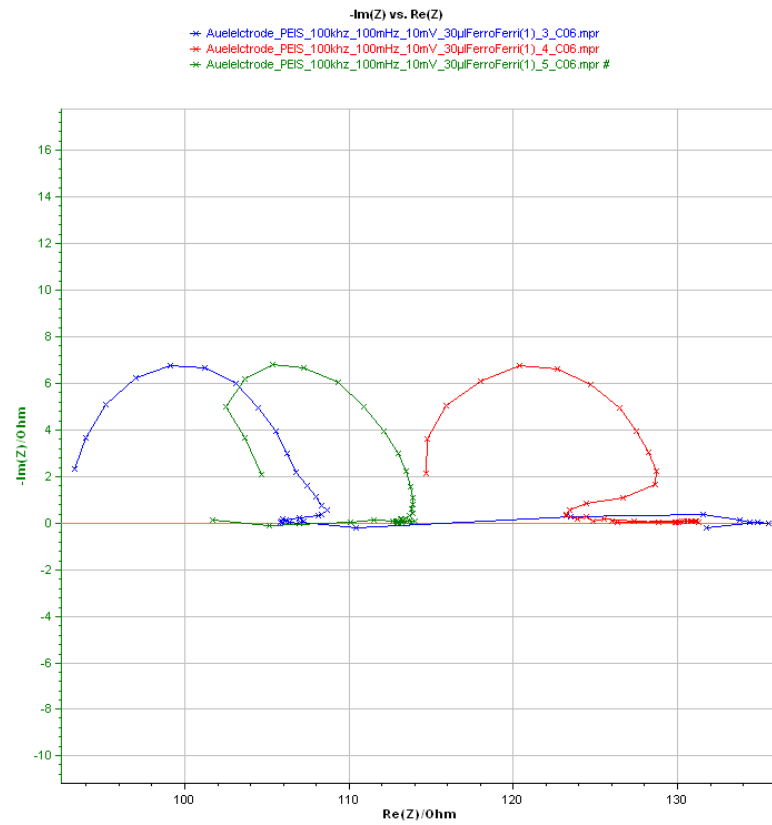


Figure 2.13: In the figure it can be seen the comparative results of the two different methods used for lift-off. In the first case (left) using an ultrasonic cleaner, it is noticeable that the result appears to be too aggressive for the electrode. The gold layer, in this case completely detaches even within the electrode shape affecting the product, while using the lab shaker (right), the method results to be conclusively more effective. The electrode is preserved in its shape and the outcome is as desired.

It also precludes the presence of a tunable Ultrasonic Cleaner in the lab, in fact working at non-settable powers, the electrode may entirely disintegrate and moreover no acceptable power range is specified in the protocol[73]. Commercially available ultrasonic devices sometimes do not have a settable power and even that changes from device to device and therefore depends on the specific device. The alternative method proposed here (figure 2.13) is based on the use of a lab shaker, micropipettes, and syringes. As the lab shaker rotates with the electrode within the

lift-off solution, an attempt is made to detach the gold by rinsing the electrode with 10-mL syringes, 20G needles and micropipettes that allow the solution to arrive with some useful pressure for detachment.

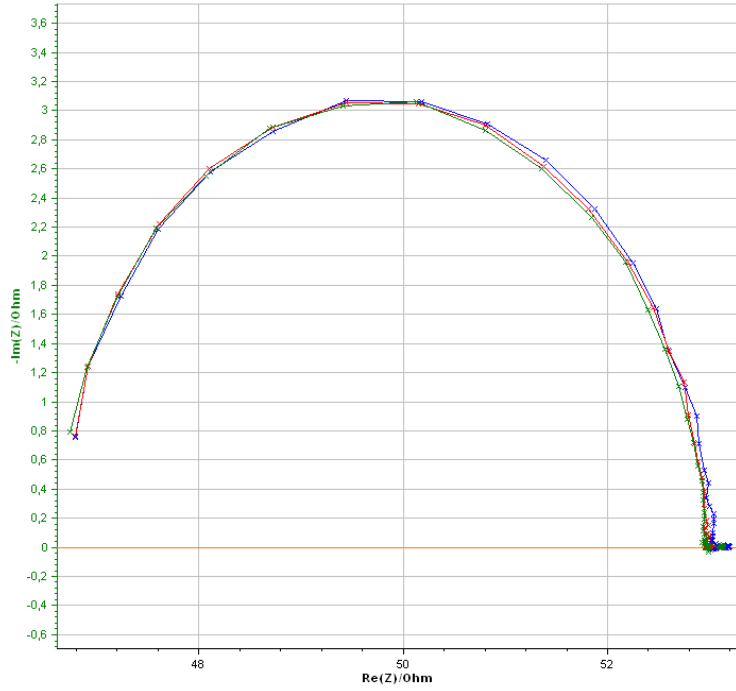
3.1.8 Electrodes Validation



Electrode Validation With Chip

-Im(Z) vs. Re(Z)

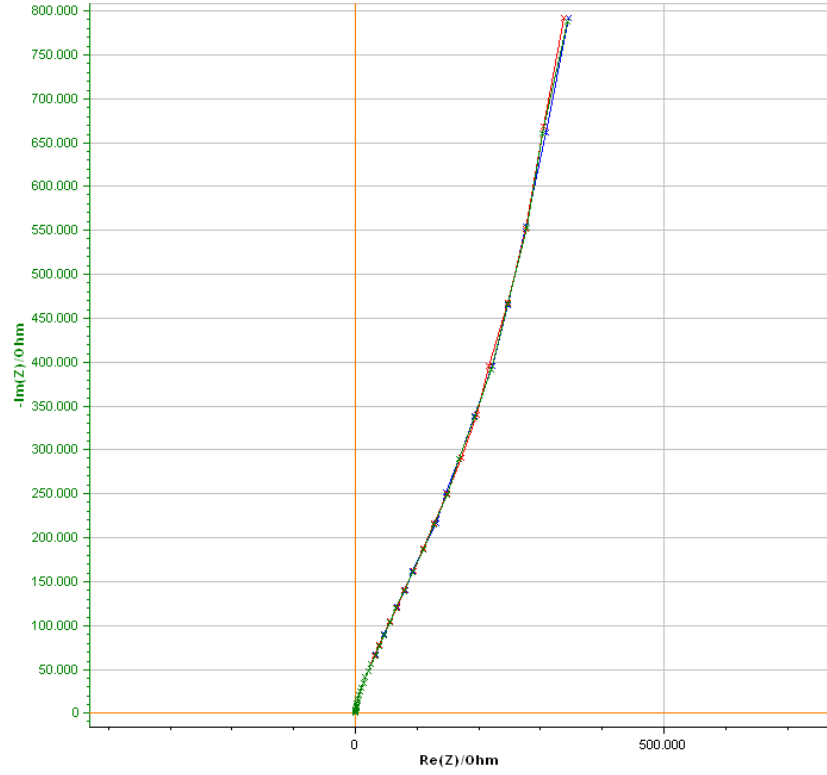
- Auelectrode_PBS_100kHz_100mHz_10mV_30uFerroFerri_10points_3drop_1_C10.mpr
- Auelectrode_PBS_100kHz_100mHz_10mV_30uFerroFerri_10points_3drop_2_C10.mpr
- Auelectrode_PBS_100kHz_100mHz_10mV_30uFerroFerri_10points_3drop_3_C10.mpr #



TEER of Cells Barrier Day3

-Im(Z) vs. Re(Z)

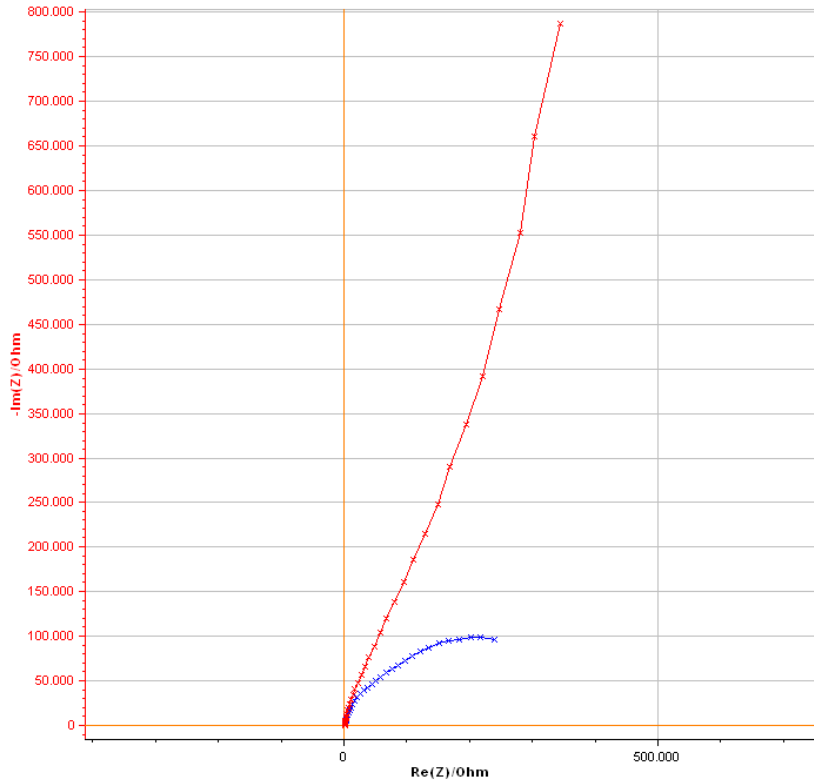
- * Auelectrode_PEIS_100khz_100mHz_10mV_MEM_day3_CH10_measure3_C10.mpr
- * Auelectrode_PEIS_100khz_100mHz_10mV_MEM_day3_CH10_measure2_C10.mpr
- * Auelectrode_PEIS_100khz_100mHz_10mV_MEM_day3_CH10_measure1_C10.mpr #



TEER of Cells Barrier Day3 Before/After Drug Addition

-Im(Z) vs. Re(Z)

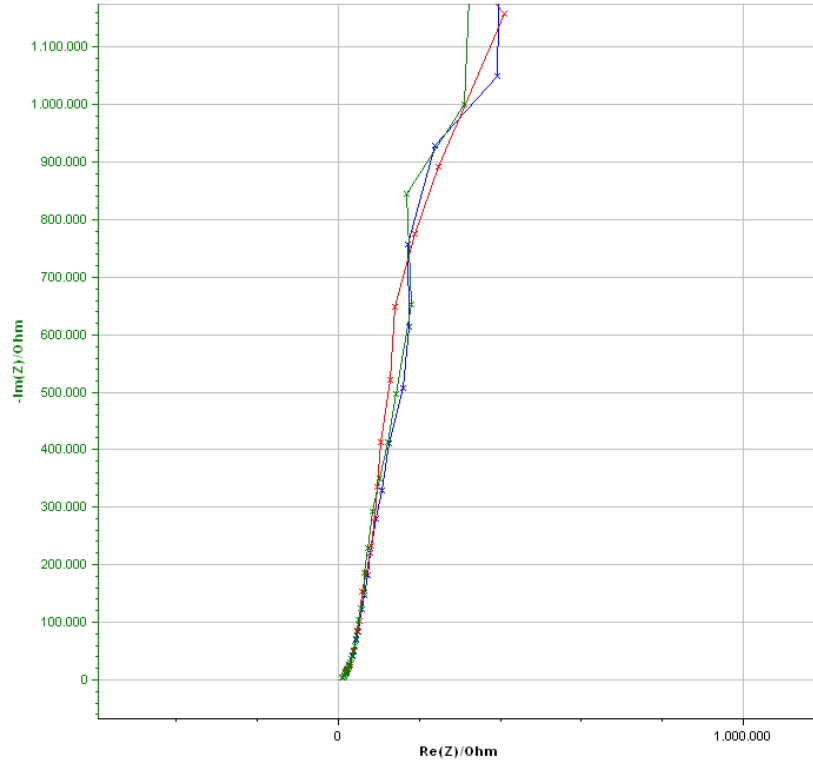
* Auelectrode_PEIS_100khz_100mHz_10mV_MEM_day3_Chip1_AfterDrug_measure1_C06.mpr
* Auelectrode_PEIS_100khz_100mHz_10mV_MEM_day3_CH10_measure1_C10.mpr #



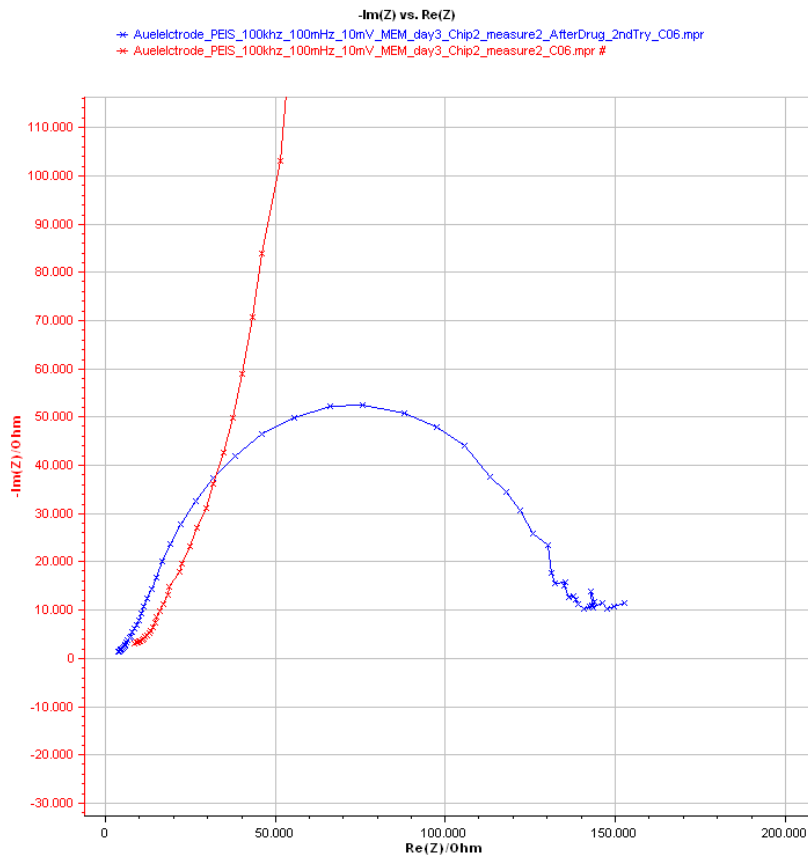
TEER Chip2 Day3

-Im(Z) vs. Re(Z)

- Auelectrode_PEIS_100khz_100mHz_10mV_MEM_day3_Chip2_measure1_C06.mpr
- Auelectrode_PEIS_100khz_100mHz_10mV_MEM_day3_Chip2_measure2_C06.mpr
- Auelectrode_PEIS_100khz_100mHz_10mV_MEM_day3_Chip2_measure3_C06.mpr #



TEER Chip2 Before/After Drug Addition



COMPARE THE PLOTS, COMBINE WITH CELLS IMAGES

TO ADD

We had to demonstrate that we can house the cells, they grow a monolayer, they form tight junctions.

If Im part of Z is higher is due to presence of cells(Increase in capacitance is related to cells and it's the Im part of Impedance)

Search something about potentiostat validation, graphic validation

Talk about different connectors used, the silver paint as well and the final easy way to test the chip without having shifting through the pogo pin.

*Show impedance graph with cells, without cells, with Crocodile, with pogo pin
And all the differences in the graphs. (proof-of-concept of electrodes)
Bode diagram, talk about the frequencies, what is the best frequency? (Around 15-40 kHz) Why?*

Talk about the compounds that was added.

3.2 Discussion

Talk about the chip that is applicable to other barriers as well

Talks about the barrier, how hard is to deal with PET very thin membrane and their integration in a chip leakage-free

How good is to have electrode on membrane, possible and future application, the need of integrated electrode in chip!

How our electrodes are now reproducible, reliable, how we create the connections with pogo-pin, the silver paint that was tried due that is very difficult to create a connection

Discuss about different photoresist that were tried, that the expired one is not working, that the Japanese one is not going to work (less redish than the other)

Talk about the 3d printed structure used for the electrodes validation.

These devices, need accurate sensors to carry out direct measurements on cell culture to be as close as possible to the in vivo organ. The sensors that are commonly integrated, however, cannot be considered 100% reliable due to large standard deviations, poor resolution, or adverse conditions during measurements. For these reasons, in this work, it is proposed the fabrication of electrodes able to perform TEER (Trans-Epithelial Electrical Resistance) measurements that allow to execute reliable impedance measurements capable of controlling the integrity of a cellular barrier with higher precision than the models on the market. The electrodes were fabricated using high-resolution photolithography process that were integrated into a previously fabricated gut-on-a-chip model to ensure their effectiveness for the final purpose.

The electrodes are fabricated directly on top of the membrane used as the intermediate layer. This represents a major innovation and considerable utility of these systems, since they are fabricated directly on the membrane, unlike the usual metal electrodes which are fabricated on glass. The manufacturing method therefore allows direct integration of the electrode into the chip. The presence of the in-situ electrodes is extremely important as it allows measurements to be made on the efficiency of the cell barrier formed during the period of cell culture inside the chip. In fact, usually the validation of the integrity of the cell barrier that has been formed during the cell culture, is carried out through open systems such as the Transwell system where cells grow in a porous membrane that is in the middle of two chambers with two independent accesses. In this case, measurements are made through chopstick electrodes introduced from outside by performing TEER measurements. Instead, the presented system in this work, allows integrity and permeability test of the barrier performing impedance measurements through electrodes integrated directly inside the chip. This allows real time measurements to be performed during the culture that takes place inside the chip and it is also

conducted in a more stable and efficient manner as the electrodes are integrated on the chip.

References

- [1] C. Rönnbäck and E. Hansson, "The importance and control of low-grade inflammation due to damage of cellular barrier systems that may lead to systemic inflammation," *Frontiers in Neurology*, vol. 10, no. MAY, 2019, doi: 10.3389/FNEUR.2019.00533.
- [2] S. Tsukita, M. Furuse, and M. Itoh, "Multifunctional strands in tight junctions," *Nat Rev Mol Cell Biol*, vol. 2, no. 4, pp. 285–293, Apr. 2001, doi: 10.1038/35067088.
- [3] S. E. Turvey and D. H. Broide, "Innate immunity," *J Allergy Clin Immunol*, vol. 125, no. 2 Suppl 2, Feb. 2010, doi: 10.1016/J.JACI.2009.07.016.
- [4] J. S. Marshall, R. Warrington, W. Watson, and H. L. Kim, "An introduction to immunology and immunopathology," *Allergy, Asthma and Clinical Immunology*, vol. 14, no. 2, pp. 1–10, Sep. 2018, doi: 10.1186/S13223-018-0278-1/TABLES/4.
- [5] Y. B. Arlik *et al.*, "Barriers-on-chips: Measurement of barrier function of tissues in organs-on-chips," *Biomicrofluidics*, vol. 12, no. 4, p. 042218, Jun. 2018, doi: 10.1063/1.5023041.
- [6] C. Förster, "Tight junctions and the modulation of barrier function in disease," *Histochemistry and Cell Biology*, vol. 130, no. 1, p. 55, Jul. 2008, doi: 10.1007/S00418-008-0424-9.
- [7] G. H. Liang and C. R. Weber, "Molecular aspects of tight junction barrier function," *Curr Opin Pharmacol*, vol. 19, p. 84, 2014, doi: 10.1016/J.COPH.2014.07.017.
- [8] I. M. Rea, D. S. Gibson, V. McGilligan, S. E. McNerlan, H. Denis Alexander, and O. A. Ross, "Age and Age-Related Diseases: Role of Inflammation Triggers and Cytokines," *Frontiers in Immunology*, vol. 9, no. APR, p. 1, Apr. 2018, doi: 10.3389/FIMMU.2018.00586.
- [9] F. A. Bonilla and H. C. Oettgen, "Adaptive immunity," *J Allergy Clin Immunol*, vol. 125, no. 2 Suppl 2, Feb. 2010, doi: 10.1016/J.JACI.2009.09.017.
- [10] E. Hansson and E. Skjödebrand, "Coupled cell networks are target cells of inflammation, which can spread between different body organs and develop into systemic chronic inflammation," *Journal of Inflammation (London, England)*, vol. 12, no. 1, Jul. 2015, doi: 10.1186/S12950-015-0091-2.
- [11] G. G. Ortiz *et al.*, "Role of the blood-brain barrier in multiple sclerosis," *Arch Med Res*, vol. 45, no. 8, pp. 687–697, Nov. 2014, doi: 10.1016/J.ARCMED.2014.11.013.
- [12] J. Cunha-Vaz, R. Bernardes, and C. Lobo, "Blood-retinal barrier," *Eur J Ophthalmol*, vol. 21 Suppl 6, no. SUPPL.6, pp. 3–9, 2011, doi: 10.5301/EJO.2010.6049.
- [13] F. Valitutti and A. Fasano, "Breaking Down Barriers: How Understanding Celiac Disease Pathogenesis Informed the Development of Novel Treatments," *Digestive Diseases and Sciences 2019 64:7*, vol. 64, no. 7, pp. 1748–1758, May 2019, doi: 10.1007/S10620-019-05646-Y.

- [14] S. Bernardo-Castro *et al.*, "Pathophysiology of Blood-Brain Barrier Permeability Throughout the Different Stages of Ischemic Stroke and Its Implication on Hemorrhagic Transformation and Recovery," *Front Neurol*, vol. 11, Dec. 2020, doi: 10.3389/FNEUR.2020.594672.
- [15] B. Srinivasan, A. R. Kolli, M. B. Esch, H. E. Abaci, M. L. Shuler, and J. J. Hickman, "TEER measurement techniques for in vitro barrier model systems," *J Lab Autom*, vol. 20, no. 2, pp. 107–126, Apr. 2015, doi: 10.1177/2211068214561025.
- [16] B. Srinivasan, A. R. Kolli, M. B. Esch, H. E. Abaci, M. L. Shuler, and J. J. Hickman, "TEER measurement techniques for in vitro barrier model systems," *J Lab Autom*, vol. 20, no. 2, pp. 107–126, Apr. 2015, doi: 10.1177/2211068214561025.
- [17] J. S. Kochhar, S. Y. Chan, P. S. Ong, W. G. Lee, and L. Kang, "Microfluidic devices for drug discovery and analysis," *Microfluidic Devices for Biomedical Applications*, pp. 231–280, 2013, doi: 10.1533/9780857097040.2.231.
- [18] R. Dorey, "Integration and devices," *Ceramic Thick Films for MEMS and Microdevices*, pp. 1–33, 2012, doi: 10.1016/B978-1-4377-7817-5.00001-8.
- [19] Steven. Saliterman, "Fundamentals of bioMEMS and medical microdevices," p. 610, 2006, Accessed: Nov. 22, 2021. [Online]. Available: https://www.researchgate.net/publication/294427683_Fundamentals_of_BioMEMS_and_Medical_Microdevices
- [20] L. R. Volpatti and A. K. Yetisen, "Commercialization of microfluidic devices," *Trends in Biotechnology*, vol. 32, no. 7, pp. 347–350, Jul. 2014, doi: 10.1016/J.TIBTECH.2014.04.010.
- [21] "Introduction to lab-on-a-chip 2020: review, history and future - Elveflow." <https://www.elveflow.com/microfluidic-reviews/general-microfluidics/introduction-to-lab-on-a-chip-review-history-and-future/> (accessed Nov. 22, 2021).
- [22] Y. B. Arlk *et al.*, "Barriers-on-chips: Measurement of barrier function of tissues in organs-on-chips," *Biomicrofluidics*, vol. 12, no. 4, p. 042218, Jun. 2018, doi: 10.1063/1.5023041.
- [23] P. Schuller *et al.*, "A lab-on-a-chip system with an embedded porous membrane-based impedance biosensor array for nanoparticle risk assessment on placental Bewo trophoblast cells," *Sensors and Actuators B: Chemical*, vol. 312, p. 127946, Jun. 2020, doi: 10.1016/J.SNB.2020.127946.
- [24] X. M. Tan and D. Rodrigue, "A Review on Porous Polymeric Membrane Preparation. Part II: Production Techniques with Polyethylene, Polydimethylsiloxane, Polypropylene, Polyimide, and Polytetrafluoroethylene," *Polymers 2019, Vol. 11, Page 1310*, vol. 11, no. 8, p. 1310, Aug. 2019, doi: 10.3390/POLYM11081310.
- [25] T. Review, H. H. Chung, M. Mireles, B. J. Kwarta, and T. R. Gaborski, "Lab on a Chip Use of porous membranes in tissue barrier and co-culture models," vol. 18, p. 1671, 2018, doi: 10.1039/c7lc01248a.

- [26] S. BOYDEN, "THE CHEMOTACTIC EFFECT OF MIXTURES OF ANTIBODY AND ANTIGEN ON POLYMORPHONUCLEAR LEUCOCYTES," *Journal of Experimental Medicine*, vol. 115, no. 3, pp. 453–466, Mar. 1962, doi: 10.1084/JEM.115.3.453.
- [27] J. J. Vandersarl, A. M. Xu, and N. A. Melosh, "Rapid spatial and temporal controlled signal delivery over large cell culture areas," *Lab on a Chip*, vol. 11, no. 18, pp. 3057–3063, Sep. 2011, doi: 10.1039/C1LC20311H.
- [28] H. H. Chung *et al.*, "Highly permeable silicon membranes for shear free chemotaxis and rapid cell labeling," *Lab on a Chip*, vol. 14, no. 14, pp. 2456–2468, Jul. 2014, doi: 10.1039/C4LC00326H.
- [29] H. J. Kim, D. Huh, G. Hamilton, and D. E. Ingber, "Human gut-on-a-chip inhabited by microbial flora that experiences intestinal peristalsis-like motions and flow," *Lab Chip*, vol. 12, no. 12, pp. 2165–2174, Jun. 2012, doi: 10.1039/C2LC40074J.
- [30] T. Bluhmki *et al.*, "Development of a miniaturized 96-Transwell air–liquid interface human small airway epithelial model," *Scientific Reports* 2020 10:1, vol. 10, no. 1, pp. 1–14, Aug. 2020, doi: 10.1038/s41598-020-69948-2.
- [31] P. Zoio, S. Lopes-Ventura, and A. Oliva, "Barrier-on-a-chip with a modular architecture and integrated sensors for real-time measurement of biological barrier function," *Micromachines (Basel)*, vol. 12, no. 7, Jul. 2021, doi: 10.3390/M12070816/S1.
- [32] G. B. Gonzales, J. van Camp, H. Vissenaekens, K. Raes, G. Smagghe, and C. Grootaert, "Review on the Use of Cell Cultures to Study Metabolism, Transport, and Accumulation of Flavonoids: From Mono-Cultures to Co-Culture Systems," *Comprehensive Reviews in Food Science and Food Safety*, vol. 14, no. 6, pp. 741–754, Nov. 2015, doi: 10.1111/1541-4337.12158.
- [33] K. Hattori, Y. Munehira, H. Kobayashi, T. Satoh, S. Sugiura, and T. Kanamori, "Microfluidic perfusion culture chip providing different strengths of shear stress for analysis of vascular endothelial function," *Journal of Bioscience and Bioengineering*, vol. 118, no. 3, pp. 327–332, Sep. 2014, doi: 10.1016/J.JBIOSC.2014.02.006.
- [34] S. Kuntz *et al.*, "Inhibition of low-grade inflammation by anthocyanins from grape extract in an in vitro epithelial-endothelial co-culture model," *Food & Function*, vol. 6, no. 4, pp. 1136–1149, Apr. 2015, doi: 10.1039/C4FO00755G.
- [35] N. Ashammakhi *et al.*, "Gut-on-a-chip: Current progress and future opportunities," *Biomaterials*, vol. 255, p. 120196, Oct. 2020, doi: 10.1016/J.BIOMATERIALS.2020.120196.
- [36] Y. B. Arlk *et al.*, "Barriers-on-chips: Measurement of barrier function of tissues in organs-on-chips," *Biomicrofluidics*, vol. 12, no. 4, Jul. 2018, doi: 10.1063/1.5023041.
- [37] W. Shin *et al.*, "A robust longitudinal co-culture of obligate anaerobic gut microbiome with human intestinal epithelium in an anoxic-oxic interface-on-a-chip," *Frontiers in Bioengineering and Biotechnology*, vol. 7, no. FEB, p. 13, 2019, doi: 10.3389/FBIOE.2019.00013/BIBTEX.

- [38] V. Berejnov, N. Djilali, and D. Sinton, "Lab-on-chip methodologies for the study of transport in porous media: energy applications," *Lab on a Chip*, vol. 8, no. 5, pp. 689–693, Apr. 2008, doi: 10.1039/B802373P.
- [39] F. Zanella, J. B. Lorens, and W. Link, "High content screening: seeing is believing," *Trends Biotechnol*, vol. 28, no. 5, pp. 237–245, May 2010, doi: 10.1016/J.TIBTECH.2010.02.005.
- [40] S. Singh, A. E. Carpenter, and A. Genovesio, "Increasing the Content of High-Content Screening: An Overview," *J Biomol Screen*, vol. 19, no. 5, pp. 640–650, 2014, doi: 10.1177/1087057114528537.
- [41] D. Marrero *et al.*, "Gut-on-a-chip: Mimicking and monitoring the human intestine," *Biosensors and Bioelectronics*, vol. 181, p. 113156, Jun. 2021, doi: 10.1016/J.BIOS.2021.113156.
- [42] K. Y. Song, H. Zhang, W. J. Zhang, and A. Teixeira, "Enhancement of the surface free energy of PDMS for reversible and leakage-free bonding of PDMS–PS microfluidic cell-culture systems," *Microfluidics and Nanofluidics 2018 22:11*, vol. 22, no. 11, pp. 1–9, Nov. 2018, doi: 10.1007/S10404-018-2152-3.
- [43] D. A. Bartholomeusz, R. W. Boutté, and J. D. Andrade, "Xurography: Rapid prototyping of microstructures using a cutting plotter," *Journal of Microelectromechanical Systems*, vol. 14, no. 6, pp. 1364–1374, Dec. 2005, doi: 10.1109/JMEMS.2005.859087.
- [44] S. Bhattacharya, A. Datta, J. M. Berg, and S. Gangopadhyay, "Studies on surface wettability of poly(dimethyl) siloxane (PDMS) and glass under oxygen-plasma treatment and correlation with bond strength," *Journal of Microelectromechanical Systems*, vol. 14, no. 3, pp. 590–597, Jun. 2005, doi: 10.1109/JMEMS.2005.844746.
- [45] M. A. Eddings, M. A. Johnson, and B. K. Gale, "Determining the optimal PDMS–PDMS bonding technique for microfluidic devices," *Journal of Micromechanics and Microengineering*, vol. 18, no. 6, p. 067001, Apr. 2008, doi: 10.1088/0960-1317/18/6/067001.
- [46] S. Li and S. Chen, "Polydimethylsiloxane Fluidic Interconnects for Microfluidic Systems," *IEEE Transactions on Advanced Packaging*, vol. 26, no. 3, pp. 242–247, Aug. 2003, doi: 10.1109/TADVP.2003.817961.
- [47] H. N. Chan, Y. Chen, Y. Shu, Y. Chen, Q. Tian, and H. Wu, "Direct, one-step molding of 3D-printed structures for convenient fabrication of truly 3D PDMS microfluidic chips," *Microfluidics and Nanofluidics*, vol. 19, no. 1, pp. 9–18, Jul. 2015, doi: 10.1007/S10404-014-1542-4/FIGURES/6.
- [48] "PDMS Molding | McGill Nanotools - Microfab." <http://mnm.physics.mcgill.ca/content/pdms-molding> (accessed Jun. 05, 2022).
- [49] Y. Hongbin, Z. Guangya, C. F. Siong, W. Shouhua, and L. Feiwen, "Novel polydimethylsiloxane (PDMS) based microchannel fabrication method for lab-on-a-chip application," *Sensors and Actuators B: Chemical*, vol. 137, no. 2, pp. 754–761, Apr. 2009, doi: 10.1016/J.SNB.2008.11.035.
- [50] F. Sassa, J. Fukuda, and H. Suzuki, "Microprocessing of liquid plugs for bio/chemical analyses," *Analytical Chemistry*, vol. 80, no. 16, pp. 6206–6213, Aug. 2008, doi: 10.1021/AC800492V.

- [51] L. Jothi and G. Nageswaran, "Plasma Modified Polymeric Materials for Biosensors/Biodevice Applications," *Non-Thermal Plasma Technology for Polymeric Materials: Applications in Composites, Nanostructured Materials, and Biomedical Fields*, pp. 409–437, Jan. 2018, doi: 10.1016/B978-0-12-813152-7.00015-9.
- [52] "Preparation of PDMS Stamps - The Odom Group." <https://www.odomgroup.northwestern.edu/pdms-stamps/> (accessed Jun. 05, 2022).
- [53] C. G. Sip and A. Folch, "Stable chemical bonding of porous membranes and poly(dimethylsiloxane) devices for long-term cell culture," *Biomicrofluidics*, vol. 8, no. 3, May 2014, doi: 10.1063/1.4883075.
- [54] B. H. Chueh, D. Huh, C. R. Kyrtos, T. Houssin, N. Futai, and S. Takayama, "Leakage-Free Bonding of Porous Membranes into Layered Microfluidic Array Systems," *Analytical Chemistry*, vol. 79, no. 9, pp. 3504–3508, May 2007, doi: 10.1021/AC062118P.
- [55] L. Tang and N. Y. Lee, "A facile route for irreversible bonding of plastic-PDMS hybrid microdevices at room temperature," *Lab on a Chip*, vol. 10, no. 10, pp. 1274–1280, May 2010, doi: 10.1039/B924753J.
- [56] "Steps for cleaning slides (a) Remove the slides from the box. (b) Clean... | Download Scientific Diagram." https://www.researchgate.net/figure/Steps-for-cleaning-slides-a-Remove-the-slides-from-the-box-b-Clean-glass-slides-and_fig1_347575944 (accessed Jun. 03, 2022).
- [57] "Ultrasonic Cleaning of Glass Slides & Vacuum Jigs - Kemet." <https://www.kemet.co.uk/blog/cleaning/ultrasonic-cleaning-of-glass-slides-and-vacuum-jigs> (accessed Jun. 03, 2022).
- [58] L. Xiong, P. Chen, and Q. Zhou, "Adhesion promotion between PDMS and glass by oxygen plasma pre-treatment," <http://dx.doi.org/10.1080/01694243.2014.883774>, vol. 28, no. 11, pp. 1046–1054, Jun. 2014, doi: 10.1080/01694243.2014.883774.
- [59] "Microfluidic interconnect by gluing tube to port, using ferrule for... | Download Scientific Diagram." https://www.researchgate.net/figure/Microfluidic-interconnect-by-gluing-tube-to-port-using-ferrule-for-improved-alignment_fig1_251343941 (accessed Jun. 06, 2022).
- [60] M. H. Zawawi *et al.*, "A review: Fundamentals of computational fluid dynamics (CFD)," *AIP Conference Proceedings*, vol. 2030, no. 1, p. 020252, Nov. 2018, doi: 10.1063/1.5066893.
- [61] D. Adechy and R. I. Issa, "Modelling of annular flow through pipes and T-junctions," *Computers & Fluids*, vol. 33, no. 2, pp. 289–313, Feb. 2004, doi: 10.1016/S0045-7930(03)00056-2.
- [62] S. E. Park, A. Georgescu, and D. Huh, "Organoids-on-a-chip," *Science (1979)*, vol. 364, no. 6444, pp. 960–965, Jun. 2019, doi: 10.1126/SCIENCE.AAW7894.
- [63] A. U. R. Aziz, C. Geng, M. Fu, X. Yu, K. Qin, and B. Liu, "The Role of Microfluidics for Organ on Chip Simulations," *Bioengineering 2017, Vol. 4, Page 39*, vol. 4, no. 2, p. 39, May 2017, doi: 10.3390/BIOENGINEERING4020039.

- [64] T. Lea, "Caco-2 cell line," *The Impact of Food Bioactives on Health: In Vitro and Ex Vivo Models*, pp. 103–111, Jan. 2015, doi: 10.1007/978-3-319-16104-4_10/FIGURES/2.
- [65] P. Artursson, K. Palm, and K. Luthman, "Caco-2 monolayers in experimental and theoretical predictions of drug transport," *Advanced Drug Delivery Reviews*, vol. 46, no. 1–3, pp. 27–43, Mar. 2001, doi: 10.1016/S0169-409X(00)00128-9.
- [66] "Morphology of Caco-2 cells cultured in the microfluidic device. Caco-2... | Download Scientific Diagram." https://www.researchgate.net/figure/Morphology-of-Caco-2-cells-cultured-in-the-microfluidic-device-Caco-2-cells-cultured-in_fig4_325071905 (accessed Jun. 10, 2022).
- [67] M. J. Briske-Anderson, J. W. Finley, and S. M. Newman, "The Influence of Culture Time and Passage Number on the Morphological and Physiological Development of Caco-2 Cells;" <https://doi.org/10.3181/00379727-214-44093>, vol. 214, no. 3, pp. 248–257, Nov. 2016, doi: 10.3181/00379727-214-44093.
- [68] D. A. Markov, E. M. Lillie, S. P. Garbett, and L. J. McCawley, "Variation in diffusion of gases through PDMS due to plasma surface treatment and storage conditions," *Biomedical Microdevices*, vol. 16, no. 1, pp. 91–96, Feb. 2014, doi: 10.1007/S10544-013-9808-2.
- [69] S. Halldorsson, E. Lucumi, R. Gómez-Sjöberg, and R. M. T. Fleming, "Advantages and challenges of microfluidic cell culture in polydimethylsiloxane devices," *Biosensors and Bioelectronics*, vol. 63, pp. 218–231, Jan. 2015, doi: 10.1016/J.BIOS.2014.07.029.
- [70] "Calcein-AM for Determination of Cell Vitality | Nexcelom Bioscience." <https://www.nexcelom.com/calcein-am-for-determination-of-cell-vitality/> (accessed Jun. 11, 2022).
- [71] "Spectrum [Ethidium Bromide] | AAT Bioquest." https://www.aatbio.com/fluorescence-excitation-emission-spectrum-graph-viewer/ethidium_bromide (accessed Jun. 11, 2022).
- [72] K. Matter and M. S. Balda, "Functional analysis of tight junctions," *Methods*, vol. 30, no. 3, pp. 228–234, Jul. 2003, doi: 10.1016/S1046-2023(03)00029-X.
- [73] P. Schuller *et al.*, "Optimized plasma-assisted bi-layer photoresist fabrication protocol for high resolution microfabrication of thin-film metal electrodes on porous polymer membranes," *MethodsX*, vol. 6, pp. 2606–2613, Jan. 2019, doi: 10.1016/J.MEX.2019.10.038.
- [74] A. J. Bard and L. R. Faulkner, "Basic Potential Step Methods," *Electrochemical Methods: Fundamentals and Applications*, pp. 156–225, Dec. 2001, Accessed: Jun. 11, 2022. [Online]. Available: <https://books.google.com.mx/books?id=kv56QgAACAAJ>
- [75] "KANOPY Crafting electrochemistry for lives..., Lab, Retail - KANOPY." <https://kanopytech.com/view/blog/convert-potentiostats-3-electrode-setup-into-2-electrode-one> (accessed Jun. 11, 2022).
- [76] A. P. Bhatt *et al.*, "Nonsteroidal Anti-Inflammatory Drug-Induced Leaky Gut Modeled Using Polarized Monolayers of Primary Human Intestinal Epithelial Cells," *ACS Infect Dis*, vol. 4, no. 1, pp. 46–52, Jan. 2018, doi: 10.1021/ACSINFECDIS.7B00139.

- [77] M. Camilleri, "The Leaky Gut: Mechanisms, Measurement and Clinical Implications in Humans," *Gut*, vol. 68, no. 8, p. 1516, Aug. 2019, doi: 10.1136/GUTJNL-2019-318427.
- [78] "Smooth Out 3D Printed Models With an Acetone Vapor Bath." <https://lifehacker.com/smooth-out-3d-printed-models-with-an-acetone-vapor-bath-1790675996/amp> (accessed Jun. 05, 2022).
- [79] "How to get a smooth finish on your castings of 3-D parts - ComposiMold.com." <https://composimoldstore.com/journal/how-to-get-a-smooth-finish-on-your-castings-of-3d-parts/> (accessed Jun. 05, 2022).
- [80] B. Y. Park, R. Zaouk, and M. J. Madou, "Fabrication of microelectrodes using the lift-off technique," *Methods Mol Biol*, vol. 321, pp. 23–26, 2006, doi: 10.1385/1-59259-997-4:23.